1   TITLE: The northern Bering Sea zooplankton community response to variability in sea ice:

2   evidence from a series of warm and cold periods

3

4

5   Author List: David G. Kimmel[1*], Lisa B. Eisner[2], and Alexei I. Pinchuk[3]

6   Author Affiliations:

7   [1] National Oceanic and Atmospheric Administration, National Marine Fisheries Service, Alaska

8   Fisheries Science Center, Seattle WA 98115, USA

9   [2] National Oceanic and Atmospheric Administration, National Marine Fisheries Service, Alaska

10   Fisheries Science Center, Juneau AK 99801, USA

11   [3] College of Fisheries and Ocean Sciences, University of Alaska Fairbanks, Juneau, AK 99801,

12   USA

13

14   *Corresponding author email: david.kimmel@noaa.gov

15

16   Running page head: Zooplankton community dynamics in the northern Bering Sea

17

18   ABSTRACT

19   Recent, unprecedented losses of sea ice have resulted in widespread changes in the northern

20   Bering Sea ecosystem and this study explores the zooplankton community response. Time-series

21   observations were used to identify zooplankton community changes in the northern ($> 60°N$)

22   Bering Sea (NBS) over a 17-year period (2002-2018). The overall objective was to determine if

23   the changes in zooplankton populations previously described for the southeastern Bering Sea

24 shelf (< 60 °N) were also observed in the NBS over alternating warm and cold periods. Particular

25 attention was paid to more recent (2014-2018) years that showed significant losses of sea ice in

26 the NBS (2017/2018) in comparison to a prior warm period (2003-2005) and an intervening cold

27 period (2006-2013). A multivariate framework (redundancy analysis) was used to explore

28 correlations with environmental conditions and differences in mean abundance across the

29 differing warm and cold periods were tested. The NBS zooplankton community had different

30 responses across each warm and cold period and the primary driver for the differences in

31 response was sea ice. Redundancy analysis demonstrated that the zooplankton community during

32 the second warm period experienced greater variability compared to the prior warm period. The

33 zooplankton community had higher abundances of small copepods and meroplankton and

34 reduced abundances of *Calanus* spp. and chaetognaths during the most recent warm period. This

35 suggested that the NBS zooplankton will not be impacted by reduced sea ice when the ice

36 coverage extends south of 60°N, but show community change once a minimum threshold in ice

37 extent and timing of retreat is reached. Shifts in the zooplankton community may have had

38 cascading effects on higher trophic levels that were evident during the latter warm period.

39

40 Keywords: Bering Sea, zooplankton abundance, zooplankton community composition, climate,

41 sea ice

42

1. INTRODUCTION

In the highly productive eastern Bering Sea ecosystem (Springer et al. 1996) the broad, shallow shelf provides a fertile ground for zooplankton production. Zooplankton form a vital link between primary producers and higher trophic levels by direct and indirect transfer of energy. Zooplankton are consumed by forage fish (Yasumiishi et al. 2020), seabirds (Piatt & Spring 2003), and marine mammals, including the critically endangered north Pacific right whale (*Eubalaena japonica*) (Baumgartner et al. 2013). Zooplankton also provide nutrition for abundant, commercially exploited fish stocks, including walleye pollock (*Gadus chalcogrammus*) and Pacific cod (*G. macrocephalus*) (Strasburger et al. 2014, Buckley et al. 2016). In the Bering Sea, much work has been done to understand the population dynamics of key zooplankton taxa that appear most frequently in higher trophic level diets. These key taxa include the predominant euphausiid species on the middle and outer shelves, *Thysanoessa raschii* and *T. inermis*, respectively (Ressler et al. 2014, Bi et al. 2015, Hunt et al. 2016) as well as the calanoid copepod *Calanus marshallae/glacialis* (Coyle & Gibson 2017, Kimmel et al. 2018, Eisner et al. 2020a). Interannual shifts in overall zooplankton community composition, in addition to changes in these key taxa, have been linked to the environmental change in the Bering Sea (Vidal & Smith 1986, Coyle et al. 2008, Eisner et al. 2014, Eisner et al. 2018). Understanding how zooplankton respond to contemporary environmental variability offers a glimpse into possible future response to predicted ecosystem change (Richardson 2008) and contribute to ecosystem-based management of fisheries.

In the eastern Bering Sea, zooplankton differ across bathymetric regions, with different communities being found in the inner (0-50 m), middle (50-100 m), and outer (100 -180 m) shelf regions (Cooney & Coyle 1982) (Fig. 1A). Differences in these communities are related to local

66 oceanography and current patterns along the shelf. In addition to spatial variability, the

67 community undergoes shifts in abundance and composition in relation to the environment.

68 Distinct zooplankton communities inhabit particular water mass types that are related to

69 atmospheric forcing and the cycle of annual ice formation and retreat (Coyle & Pinchuk 2002,

70 Eisner et al. 2018, Kimmel et al. 2018). Most often compared are warm years characterized by

71 early ice retreat, a later spring phytoplankton bloom, and higher overall temperatures; and cold

72 years characterized by late ice retreat, an earlier ice-associated bloom, and lower overall

73 temperatures (Hunt et al. 2011) . In the southeastern Bering Sea, *Calanus* spp. populations have

74 reduced abundance and lower lipid content during warm periods in contrast to colder years that

75 have increased abundance, persistence on the shelf into fall, and higher lipid content (Heintz et

76 al. 2013, Eisner et al. 2018, Kimmel et al. 2018).

77   The northern Bering Sea (NBS) shelf is characterized by seasonal sea ice cover and high

78 water column production that typically goes ungrazed resulting in tight benthic pelagic coupling

79 (Grebmeier 2012). The region also has reduced salinities at the surface, cold bottom

80 temperatures, and a stronger pycnocline compared to the southern shelf (Stabeno et al. 2012a).

81 Three water mass types predominate in the NBS: Anadyr Water that is cold, saline, and nutrient-

82 rich and found in the western, outer shelf and north of St. Lawrence Island; Alaska Coastal

83 Water that is warmer and fresher found near the Alaskan coast; and Bering Shelf Water that is

84 intermediate in salinity and temperature (Coachman et al. 1975). Danielson et al. (2017) has

85 noted the role that seasonality plays in influencing these water masses and winds may redirect

86 typical flow patterns during particular times of the year with not well-understood biological

87 consequences (Danielson et al. 2017, Eisner et al. 2020b). Differences among fauna are related to

88 these differences in hydrography (Siddon et al. 2020) and zooplankton show correlations to

89   particular water masses or temperature and salinity characteristics (Eisner et al. 2013, Pinchuk &

90   Eisner 2017). These correlations appear to be robust and have been tracked as water moves into

91   the Chukchi Sea (Hopcroft et al. 2010, Ershova et al. 2015, Kim et al. 2020).

92   The NBS was predicted to remain strongly influenced by persistent seasonal ice cover

93   (Hermann et al. 2016), albeit with interannual variability until at least 2050 (Stabeno et al.

94   2012a). However, recent years of unprecedented low ice coverage have occurred, resulting in

95   shifts in oceanographic conditions across the NBS (Stabeno & Bell 2019, Basyuk & Zuenko

96   2020) that have been linked to ecosystem-wide responses (Duffy-Anderson et al. 2019, Siddon et

97   al. 2020). The recent low ice event of 2018 was determined to be the lowest ice extent in the last

98   5500 years based on peat cellulose oxygen isotopes from St. Matthew Island (Jones et al. 2020).

99   Most notable was the significant reduction in cold pool (< 2 °C bottom water) extent (Stabeno &

100   Bell 2019) and weakened stratification (Duffy-Anderson et al. 2019). This was related to a

101   delayed spring phytoplankton bloom (Kikuchi et al. 2020) and a shift in phytoplankton (Fukai et

102   al. 2020) and zooplankton community composition (Kim et al. 2020, Kimura et al. 2020). Other

103   ecosystem effects were also noted, including: northward movement of demersal fish populations

104   (Stevenson & Lauth 2018, Eisner et al. 2020b), shifts in spatial location of forage fish

105   (Yasumiishi et al. 2020), sea-bird die-offs (Romano et al. 2020, Will et al. 2020), poor body

106   condition of seals (Boveng et al. 2020), and an Unusual Mortality Event was declared for

107   bearded, ringed, and spotted seals (Boveng 2019).

108   Past studies of the NBS focused on short time frames of zooplankton distributions in

109   relation to water mass characteristics (Eisner et al. 2014, Yamaguchi et al. 2021). Here, we seek

110   to build on these studies and provide a time-series perspective of how the NBS zooplankton

111   community changed over a 17-year period (2002-2018) in response to alternating warm and cold

112   periods (Duffy-Anderson et al. 2017, Duffy-Anderson et al. 2019). The extremely low ice cover

113   in the winters of 2017/2018 and 2018/2019 suggests warming may be occurring more rapidly in

114   the NBS than has been predicted. The overall objective of this study was to determine if the

115   changes observed in zooplankton populations in the southeastern Bering Sea also occurred in the

116   NBS over this period of changing climate conditions (warm, cold, warm). We focused on

117   comparing the zooplankton response of the more recent years with minimal ice cover (Stabeno &

118   Bell 2019) to that of a prior warm period to determine if warm period responses were similar.

119   We chose to examine the zooplankton variability in a multivariate framework to discover overall

120   community patterns and then chose to focus on individual taxa belonging to specific groups.

121   Understanding the zooplankton community response to short-term warming events may provide

122   a window into predicting the future community structure and function in a warmer Bering Sea

123   and its impact on the broader ecosystem.

124

125   2. MATERIALS & METHODS

126   2. 1 Study area

127   Based on physics and biology, Stabeno et al. (2012a) placed the dividing line between the

128   northern and southern Bering Sea at 60°N. The northern Bering Sea is seasonally covered in ice

129   with maximum extent occurring between January and May, but typically peaking in March

130   (Clement Kinney et al. 2022), with ice extending south of 60°N (Stabeno et al. 2012a). The

131   northern Bering Sea shelf is typically ice free by June and the retreating ice leaves behind a large

132   region of bottom water < 2 °C referred to as the cold pool (Clement Kinney et al. 2022) that can

133   extend well into the southeastern Bering Sea. As ice melts and the region warms, the

134   southeastern Bering Sea middle shelf region stratifies resulting in a two layer system with a

135   mixed layer depth of approximately 25-30 m (Danielson et al. 2011, Stabeno et al. 2012a). This

136   stabilization of the water column results in the spring phytoplankton bloom (Danielson et al.

137   2011, Sigler et al. 2014). The inner shelf remains vertically mixed or only partially stratified and

138   a sharp transition occurs between the inner and middle shelf waters known as the inner front

139   which occurs at or near the 50 m isobath (Stabeno et al. 2001). This inner front often prevents the

140   movement of low salinity water onto the middle shelf, but may be eroded by winds resulting in

141   cross-shelf transport. Danielson et al. (2011) notes that this cross-shelf transport is impacted by

142   the relative location of the Aleutian Low either trapping waters near the coast or advecting them

143   onto the middle shelf. As previously mentioned, the zooplankton community differs across the

144   inner (0-50 m), middle (50-100 m), and outer (100 -180 m) shelf regions (Fig 1A). These cross-

145   shelf regions are less pronounced north of 60°N; however, the inner-front was reported as

146   occurring along the 50 m isobath north of Nunivak Island (Coachman 1986).

147   We focused on the middle and inner shelves as the outer shelf region had few samples for

148   comparison. We used the polygons developed by Ortiz et al. (2012) to define the inner shelf

149   using North Inner Shelf region (Ortiz et al. region 11) and the middle shelf as a combination of

150   St. Matthews (Ortiz et al. region 9) and North Middle Shelf regions (Ortiz et al. region 10). (Fig.

151   1A). Zooplankton and CTD sampling varied within each region (Fig. 1B), but total stations

152   occupied were similar between the two regions: middle (370 total stations) and inner (394 total

153   stations) shelves. As is common with ecological data, stations often had missing data, thus the

154   total sample number reported in the analysis is less than these totals. We also chose to group

155   years together to reflect the current temporal occurrence of multiple warm or cold years in a row

156   (Duffy-Anderson et al. 2017). We divided the time-series into three distinct periods: Warm 1

157   (2002-2005), Cold (2006-2013), and Warm 2 (2014-2018) based on cold pool area (see below).

158

159 2.2 Environmental data

160   Climate and environmental variables are listed in Table 1. The Arctic Oscillation (AO)

161 index is obtained by projecting the AO loading pattern to the daily anomaly 1000 mb height field

162 over 20°N-90°N latitude (Thompson & Wallace 1998). Here we show the index as a mean of the

163 November through March values as this period is the most influential in terms of ice formation.

164 We also evaluate the North Pacific Index (NPI), an indicator of the Aleutian Low, since

165 atmospheric phenomena over the Arctic (AO index) and Gulf of Alaska (NPI) can impact the

166 NBS region (Trenberth & Hurrell 1994). Southeast (SE) and Northwest (NW) winds are the

167 proportion of daily NCEP/NCAR Reanalysis wind data at 60°N 170°W blowing from each

168 direction. These are used as an index for shifts in Bering Sea advection (Danielson et al. 2012).

169 We report wind speed (m s^{-1}) anomalies from two time periods: February-May (spring) which

170 covers the early season of zooplankton growth and production and the June-September (summer)

171 period preceding and during the sampling period for zooplankton. Finally, we compute a wind

172 mixing index for June-September by taking the cube of the time-period mean u wind component

173 at 60°N 170°W, since the cube of the friction velocity (u) is proportional to the rate of

174 mechanical energy translated to mixing at the ocean surface (Bond & Adams 2002).

175   Total ice-covered area (km^2) from January through April for the entire Bering Sea (south

176 of Bering Strait) was acquired from the National Snow and Ice Data Center. A pixel was

177 considered ice-covered if the ice cover exceeded 15%. This cut-off was also used to estimate

178 time-period average or annual ice-extent on 15 March. A more localized picture of the ice

179 coverage was obtained from the M8 mooring site where a sea-ice profiler allows the percent ice

180 cover to be estimated (Stabeno et al. 2019) and we report this percentage for March. Summer

181   cold pool extent measures the area (km^2) of cold ($< 2°C$) bottom water that persists on the Bering

182   Sea shelf after ice retreat (Stabeno et al. 2001) and is associated with zooplankton variability

183   (Thorson et al. 2020). We report values calculated after the methods of Fedewa et al. (2020) and

184   use bottom temperature data collected by the Alaska Fisheries' Science Center (AFSC) bottom

185   trawl survey (Table 1). The 2°C isotherm from these data was also used to estimate time-period

186   average or annual cold pool extent. The degree of total ice cover, wind direction and strength,

187   and wind mixing impacts advection and timing of the spring phytoplankton bloom, which

188   precedes the sampling of zooplankton populations in this study by 2-5 months (Stabeno et al.

189   2001, Nielsen et al. 2020).

190   Water temperature and salinity data were calculated from conductivity-temperature-

191   depth (CTD) measurements (Sea-Bird (SBE) 911 or SBE25 CTD) made immediately prior to

192   zooplankton sampling. The mean temperature and salinity above and below the surface mixed

193   layer depth (MLD) was estimated at each station following Danielson et al. (2011) who defined

194   the MLD as the depth where σ_t is 0.10 kg m^{-3} greater than the value at 5 m depth. We did not

195   compute MLD for the inner shelf as many of the stations were shallow and completely mixed.

196

197   2.3 Phytoplankton data

198   Water samples for total and size fractionated chlorophyll *a* (Chl *a*) were collected with

199   Niskin bottles attached to the CTD. Samples were filtered through Whatman GF/F filters

200   (nominal pore size 0.7 μm) to estimate total Chl *a*, and through polycarbonate filters (pore size

201   10 μm) to estimate large-size fraction Chl *a*. Filters were stored frozen at -80°C and analyzed

202   within 6 months with a Turner Designs benchtop fluorometer following standard acidification

203   methods (Parsons et al. 1984).

204

2.4 Zooplankton data

Zooplankton were collected using multiple gear types over the sampling period (Table 2). Smaller zooplankton were collected using a vertically towed Juday net (37 cm diameter, 168 μm mesh) (Shevelev 2004) from 2002 to 2011 and paired bongo nets (20 cm frame, 153 μm mesh for the smaller net) (Kimmel et al. 2018) from 2012 to 2018. Larger zooplankton were collected with an obliquely towed ring net (60 cm diameter, 505 μm mesh) from 2002 to 2011 for a subset of the samples and obliquely towed, paired bongo nets (60 cm frame, 505 μm mesh) for the majority of the samples. The mesh size (505 μm) and diameter (60 cm) was the same for the ring net and the bongo net and they were deployed in the same manner (oblique tow at 0.5-0.75 m s^{-1}) and we assumed these gears were comparable. A comparison of zooplankton abundance estimated from the different smaller mesh size gear deployed at the same location across two surveys conducted in the Chukchi Sea (Figure S1) is presented in the Supplementary Materials. This comparison provides context for how these nets compared when deployed at the same location. Based on these comparisons, we suggest that the two gear types are comparable for most taxa, showing increases and decreases in abundance that covary (Figs. S2-8). Additional information on gear comparisons may be found in Gorbatenko and Dolganova (2007). Vertical tows were within 5 m off the bottom and oblique tows were within 5-10 m of the bottom depending on sea state. Volume filtered was estimated from the distance (depth) towed for the Juday net assuming 100% filtering efficiency and using a General Oceanics flowmeter mounted inside the mouth of each net for the 60 cm diameter nets. Filtration efficiency may vary considerably due to particle concentration, mesh size, diameter, and length of net (Skjoldal et al. 2019). Samples were preserved in 5% buffered formalin/seawater.

10

227   Zooplankton were identified to the lowest taxonomic level and stage possible at either the

228   University of Alaska Fairbanks, the Plankton Sorting and Identification Center (PSIC) in

229   Szczecin, Poland, and onboard ship (Juday net samples) by taxonomists from the Pacific Branch

230   of the Russian Federal Research Institute of Fisheries and Oceanography (TINRO). Samples

231   identified at the PSIC were verified at the AFSC, Seattle, Washington, USA. Hereafter, we will

232   refer to *Calanus marshallae/glacialis* as *Calanus* spp. as the ability to distinguish between these

233   sibling species morphologically is based on taxonomic characters that require significant

234   processing time (Frost 1974). This appears to be a problem across the genus as it has been

235   suggested that the ability to distinguish between *C. glacialis* and *C. finmarchicus* in Atlantic

236   waters can only be accomplished with DNA methods (Choquet et al. 2018). Recent results

237   suggest that most *Calanus* in the Bering Sea may in fact be *glacialis* (Tarrant et al. 2021);

238   however, these data are from one year only, so we will refer to *Calanus* spp. in this paper. We

239   selected the taxa for inclusion in the analysis by ranking each taxa according to its percent

240   contribution to the total abundance for each sample and each gear type. We estimated the percent

241   contribution for each taxa across the entire data set and chose those taxa that made up at least 5%

242   of the total abundance on average (Table 3). We also grouped each individual taxa into a broader

243   group for easier interpretation of the results. The four groups were: Copepods > 2 mm as adults,

244   Copepods < 2 mm as adults, other holoplankton, and meroplankton (Table 3). It is important to

245   note that a constituent of the zooplankton community, euphausiids, do not have abundance

246   estimates reported here, as larger euphausiids are able to effectively avoid capture (Sameoto et

247   al. 1993) thereby making euphausiid abundance estimates semi-quantitative. Accurate and

248   precise measurements of euphausiid abundances in the Bering Sea remain the subject of debate

249   (Hunt et al. 2016).

250

2.5 Statistical analysis

All statistical analyses were performed within the R computing environment, version 3.5.0 (R Core Team 2019). We compared average conditions across each of the three warm or cold time-periods using either one-way ANOVA with the *anova* function, *stats* package or Kruskal-Wallis test (Kruskal & Wallis 1952) with the *kruskal.test* function, *stats* package. Prior to performing the comparison, the data were tested for normality using the Shapiro-Wilk test (Shapiro & Wilk 1965) with the *shapiro.test* function, *stats* package and homogeneity of variances using the Levene test (Levene 1965) with the *leveneTest* function, *car* package (Fox & Weisberg 2019). If neither assumption was violated, we used a one-way ANOVA and tested for post-hoc differences using Tukey's Honest Significant Difference test (Tukey 1949) with the *TukeyHSD* function, *stats* package. If an assumption was violated, we used Kruskall-Wallis and tested for post-hoc differences using Dunn's test (Dunn 1964) with the *dunn.test* function, *dunn.test* package (Dinno 2017).

We conducted a multivariate, redundancy analysis (RDA) (Borcard et al. 2011) using the *rda* function in the *vegan* package (Oksanen et al. 2019). We combined all taxa abundance estimates into the RDA, regardless of net size. Data were standardized prior to analysis using the *decostand* function in the *vegan* package using the "range" method (Borcard et al. 2011). RDA included a stepwise-model selection step (*ordistep* function in *vegan* package) to identify variables for inclusion into the RDA model at a cutoff value of ($p < 0.05$). Comparison of total model fit was done using an Akaike Information Criterion (AIC) and the model with the lowest AIC was considered the best fit. We also performed correlation analyses between environmental variables and zooplankton abundances using the *cor* function in the *stats* package.

273

3. RESULTS

3.1 Environment

The area of the Bering Sea covered by ice was less in both warm periods compared to the cold period (Fig. 1C, Fig. 2A, B) and was markedly reduced in 2018 with maximum extent occurring north of 60°N (Fig. 1C). Both warm periods differed from the cold period, but not from each other in terms of total ice area or ice cover (Fig. 2A, B). Cold pool was also reduced in both warm periods (Fig. 2C) and the cold pool extended much further south, on average, during the cold period (Fig. 1D). As with ice, the cold pool area differed between warm and cold periods, but not when comparing the two warm periods (Fig. 2C). The two climate indices, the Arctic Oscillation, North Pacific Index, wind mixing, and seasonal wind speeds showed variability over the warm and cold periods (Fig. S9), but did not differ on average (data not shown).

Mixed layer depth (MLD) was reduced during the cold period on the middle shelf (Fig. 3A) and only the second warm period had deeper MLD than the cold period (Fig. 3A). Surface temperatures did not differ between the first warm period and the cold period, but both of these periods were statistically different from the higher temperatures that occurred in the second warm period (Fig. 3B, C). Bottom temperatures anomalies differed across all three time-periods on the middle shelf (Fig. 3D), but only the cold period differed from the warm periods on the inner shelf (Fig. 3E). As with bottom temperature, surface salinity differed across all three time periods on the middle shelf (Fig. 3F), whereas only the two warm periods differed on the inner shelf (Fig. 3G). Bottom salinities did not differ between any time period (Fig. 3H, I).

295

296   3.2 Phytoplankton

297   All three time-periods differed in total Chl *a* concentration on the middle shelf with time-

298   period average concentrations declining over time (Fig. 4A). The same decline was observed on

299   the inner shelf, but only the first warm period differed in average concentration from the cold

300   period (Fig. 4B). Chl *a* concentration anomalies for cells > 10 μm in size mirrored the variability

301   in total Chl *a* concentration over time and resulted in significant differences across all three time

302   periods in both shelf regions (Fig. 4C, D). The proportion of Chl *a* found in cells > 10 μm in size

303   was highest in the first warm period and declined over time on both the middle and inner shelves

304   and all three time periods also differed in the average proportion of cells > 10 μm in size (Fig.

305   4E, F).

306

307   3.3 Zooplankton

308   3.3.1 Redundancy analysis

309   Redundancy analysis showed associations between environmental variables and

310   zooplankton abundance in both shelf regions. The best fit model identified by stepwise selection

311   for the middle shelf had ice area, Total Chl *a*, Chl *a* > 10 μm in size, cold pool extent, M8 ice

312   cover, and bottom temperature as the variables correlated with zooplankton community

313   variations (Table 4). Ice area was the first variable loaded into the model and explained the

314   majority of the variance (Table 4). Similarly, the best fit model identified by stepwise selection

315   for the inner shelf had M8 ice cover, bottom temperature, ice area, and cold pool extent (Table

316   4). M8 ice cover was the first variable loaded into the model and explained the majority of the

317   variance (Table 4).

318

319   3.3.2 Copepods > 2 mm

320   The three larger species of copepods showed differing responses to environmental

321   variability. *Calanus* spp. (CA) was negatively associated with bottom temperature and positively

322   associated with cold pool area (Fig. 5A, 6A). The correlation heat map showed *Calanus* spp. was

323   positively correlated to ice area, M8 ice, and cold pool area on both shelves and the opposite

324   correlation patterns were observed for *Epilabidocera* and *Tortanus* (Fig. 7). All three periods had

325   different, average *Calanus* spp. abundances with the first warm period having the lowest

326   abundances, followed by the second warm period, and the cold period (Fig. 8A, B). Both

327   *Epilabidocera longipedata* (EP) and *Tortanus discaudatus* (TO) had positive association with

328   bottom and surface temperature and total Chl *a* concentration in both shelf locations (Fig. 5A,

329   6A). *Epilabidocera* was nearly absent from the plankton during the first warm and cold periods

330   (Fig. 8C, D); however, was found in high abundances during the second warm period (Fig. 8C,

331   D). *Tortanus* abundance was low on the middle shelf overall and was highest during the first

332   warm period (Fig. 8E) in contrast to the inner shelf where abundances were higher overall and

333   highest during the second warm period (Fig. 8F).

334

335   3.3.3 Copepods < 2 mm

336   *Acartia* spp. (AC) was associated with colder conditions, in contrast with *Centropages*

337   *abdominalis* (CE), *Oithona* spp. (OI), and *Pseudocalanus* spp. (PS) which were associated with

338   warmer conditions (Fig 5B, 6B). Correlations for these species were strongest on the inner shelf

339   and weaker on the middle shelf as indicated by the correlation heat map (Fig. 7). Positive

340   correlations were found between ice area, M8 ice cover and cold pool area for *Acartia* spp. on

341   both shelves (Fig. 7). Negative correlations for these same variables were observed on both

shelves for *Centropages* and *Oithona* spp. (Fig. 7). *Pseudocalanus* spp. had weak correlations on the middle shelf, but strong, negative correlations to ice area and M8 ice on the inner shelf (Fig. 7). *Acartia* abundances showed only a slight increase during the second warm period on the middle shelf (Fig. 9A) and higher, average abundances after the first warm period on the inner shelf (Fig. 9B). *Centropages* average abundances remained low on the middle shelf, with more individuals present during the first warm period (Fig. 9C); however, significant increases in mean abundance were observed in both warm periods on the inner shelf (Fig. 9D). *Oithona* spp. mean abundance was only elevated during warm periods on the middle shelf (Fig. 9E), but the inner shelf populations did not differ (Fig. (F). *Pseudocalanus* spp. had the highest, mean abundance during the second warm period in both shelf locations (Fig. 9G, H).

3.3.4 Other Holoplankton

Other holoplankton taxa showed less variability overall compared to copepods and meroplankton (Fig. 5C, 6C). Correlations with environmental variables were near zero for other holoplankton on the middle shelf and were stronger on the inner shelf (Fig. 7). Amphipoda (AM) showed no consistent relationship with environmental condition based on the RDA analysis (Fig. 5C, 6C) and on average, abundances remained similar across warm and cold periods (Fig. 10A, B). The exception was two abundances peaks (Fig. S14) that caused average abundances to be higher on the middle shelf in the second warm period (Fig. 10A) and inner shelf in the cold period (Fig. 10B). The peak on the inner shelf occurred during the cold period and thus resulted in positive correlations with cold conditions (Fig. 7). Based on the RDA, Appendicularia (AP) was associated with warmer conditions (Fig 5C, 6C) and correlations between bottom temperatures were positive and correlations between ice area, M8 ice, and cold pool area were

365   negative on both shelves (Fig. 7). Appendicularia mean abundance was highest during the

366   second warm period on both shelves (Fig. 10C, D), but was also elevated on the middle shelf

367   during the cold period (Fig. 10C). Chaetognatha (CH) was associated with colder conditions

368   (Fig. 5C, 6C) and had positive correlations with ice area, M8 ice cover, and cold pool area and

369   negative correlations with bottom (Fig. 7). Chaetognatha mean abundances were consistently

370   higher during cold periods (Fig. 10E, F). Similar to Amphipoda, Cnidaria (CN) and *Limacina*

371   *helicina* (LH) had no consistent association with environmental variables in the RDA (Fig. 5C,

372   6C). On the middle shelf, Cnidaria was negatively correlated with cold conditions in contrast

373   with *Limacina helicina* (LH), which was positively correlated with cold conditions (Fig. 7).

374   These relationships were opposite on the inner shelf for Cnidaria, which was positively

375   associated with cold conditions (Fig. 7). Cnidaria abundances were higher during warm periods

376   on average (Fig. 10G, H), excepting the second warm period on the outer shelf (Fig.10G) and

377   *Limacina* did not differ across warm and cold periods in either shelf location (Fig. 10I, J).

378

379   3.3.5 Meroplankton

380   The three meroplankton groups had weaker associations with environmental variables on

381   the middle shelf (Fig. 5D) compared to the inner shelf (Fig. 6D).The strongest relationships were

382   found for Bivalvia (BI), which had negative correlations with ice area, M8 ice, and cold pool

383   area and positive correlations with bottom temperature (Fig. 7). Cirripedia (CI) and Polychaeta

384   (PO) also had positive correlations with bottom temperature (Fig. 7), but the correlations

385   between ice and cold pool area were not consistent across shelves for Polychaeta (Fig. 7).

386   Average abundances of Bivalvia were lowest on the middle shelf during the cold period (Fig.

387   11A) and highest on the inner shelf in the second warm period (Fig. 11B). Cirripedia average

388   abundances were highest during first warm period on the middle shelf (Fig. 11C) and equally as

389   high during both warm periods on the inner shelf (Fig. 11D). Average Polychaeta abundance was

390   lower on the middle shelf overall, but highest during the two warm periods (Fig. 11E). Higher

391   abundances of Polychaeta were observed on the inner shelf and abundances during the cold and

392   second warm period were higher than those of the first warm period (Fig 11F).

393

394

395   4. DISCUSSION

396   The northern Bering Sea (NBS) zooplankton community had different responses across

397   each warm and cold period. We attribute the difference in response was to sea ice, the primary

398   variable identified in the redundancy analysis for both shelf regions (Table 4). Of particular note

399   was the dramatic reduction in sea ice observed in the second warm period (Fig. 1C) (Stabeno &

400   Bell 2019). Warm periods were characterized by reduced ice area and ice cover (Fig. 2A, B) that

401   resulted in a reduction in cold pool area (Fig. 1D; Fig. 2C), positive temperature anomalies (Fig.

402   3B-E), and a shift to smaller phytoplankton cells (Fig. 4), though this occurred only in the second

403   warm period (Eisner et al. 2019, Siddon et al. 2020). Redundancy analysis demonstrated that the

404   zooplankton community during the second warm period experienced greater variability

405   compared to the prior warm period as given by the wider spread of points in the RDA analyses

406   (red squares, Figs. 5 and 6). This suggests that the when the ice coverage extends south of 60°N,

407   as was observed in 2002-2005 (Fig. 1C), the NBS zooplankton community will less impacted.

408   Once a minimum threshold in ice extent and timing of retreat is reached, as happened during the

409   second warm period (Fig. 1C), the community will show a response. In general, Copepods < 2

410   mm (except *Acartia* spp.), Meroplankton, and Copepods > 2 mm (except *Calanus* spp.)

18

411   abundance were all negatively correlated with colder conditions and positively correlated with

412   warm conditions, in particular bottom temperature (Fig. 7). These local responses may be

413   significantly altered by advection, though we found no relationships with wind in this study as

414   our proxy for advection. Cold years with ice-cover in the NBS may have experienced less

415   advection of zooplankton populations into these waters resulting in less overall variability in the

416   zooplankton community, whereas warm years saw zooplankton populations advected into this

417   region. This is supported by the observation that heat flux advection increased dramatically

418   during 2014-2018 in the northern Bering and Chukchi Seas (Danielson et al. 2020). The shifts in

419   the zooplankton community that we observed (e.g., an increase in smaller-sized copepods, neritic

420   species, and meroplankton) may have contributed to the ecosystem response seen in higher

421   trophic level organisms, such as seabird die-offs, as described in Siddon et al. (2020).

422   Both warm periods differed from the cold period in average ice area and cover as well as

423   cold pool extent, but the two warm periods did not differ statistically (Fig. 2). The lack of

424   statistical difference was directly related to the impacts of the 2017/2018 winter on both ice and

425   cold pool extent, increasing the magnitude of the standard deviation for these metrics for the

426   second warm period. The NBS near M8 has experienced considerable variability in the timing of

427   sea ice arrival/retreat over time, but it was largely ice covered for approximately five months of

428   the year (Stabeno & Bell 2019, Stabeno et al. 2019). This changed in 2017/2018 with a late

429   arrival and early retreat of the ice that was driven by shifts in wind (in particular, strong winds

430   from the south during February) (Stabeno & Bell 2019, Thoman et al. 2020). We found no

431   differences in spring or summer wind speed or mixing across time periods likely because we

432   averaged wind speeds and mixing over discrete time-periods, rather than examine daily wind

433   variability within a given year. The cold pool area was larger, on average, in the second warm

434   period (Fig. 2), but again this masked the smallest ever recorded cold pool extent in 2018

435   (Stabeno & Bell 2019) and the 2°C isotherm was not detected in the bottom trawl survey during

436   2018 (Fig. 1 D). We could have separated the years 2017 and 2018 into a third warm period to

437   explore these differences however, the resulting sample size would have been too small for

438   meaningful statistical comparison. We also suspect that a finer spatially resolved ice coverage

439   index, rather than a Bering Sea-wide annual index, would show greater differences for the NBS

440   in the second warm period and we aim to explore this in a future study. We conclude that the

441   warm periods present in this data set were similar in terms of average annual indices overall, but

442   note that the winter of 2017/2018 distorted the averages reported here as defining a "warm"

443   period. The winter of 2017/2018 represented a significant anomalous event resulting in large

444   shifts in oceanographic conditions as has been widely reported (Stabeno & Bell 2019, Siddon et

445   al. 2020).

446   The two warm periods had different water column characteristics relative to the cold

447   period, and these also differed between the two shelf regions. The early ice retreat on the middle

448   shelf resulted in increased mixing of more saline bottom waters with fresher water left after ice

449   retreat, resulting in a greater MLD and higher salinities at the surface (Danielson et al. 2011).

450   Temperatures increased in both surface and bottom waters during both warm periods, with the

451   notable exception of the middle shelf during the first warm period, which had lower average

452   surface temperature relative to the subsequent cold period (Fig. 3B). Bottom temperatures were

453   much warmer on the middle shelf in the first warm period relative to the other time periods (Fig.

454   3). This difference in surface and bottom warming over contrasting warm and cold periods has

455   been noted (Stabeno et al. 2012b) as stratification differences do not always impact bottom

456   temperatures in a consistent manner (Ladd & Stabeno 2012). This highlights the difficulties in

20

457   ascribing "warm" and "cold" to particular time periods based solely on temperature in these

458   layers. The salinity response also differed between the middle and inner shelves at the surface,

459   with salinities increasing during warm periods on the middle shelf (Fig. 3F) and decreasing on

460   the inner shelf, though only in the second warm period (Fig. 3G). In contrast, the inner shelf was

461   influenced by increased freshwater input as a result of warmer conditions, thus lower salinity

462   waters left by retreating ice remained reduced in salinity (Ueno et al. 2020). This led to an

463   inverse correlation between surface salinities on the middle and inner shelves (Danielson et al.

464   2011).

465   Total chlorophyll a and chlorophyll $a > 10$ μm concentrations, as well as the proportion

466   of cells > 10 μm, were all highest in the first warm period (Fig. 4). We expected both warm years

467   to be characterized by smaller cell sizes due to the tendency for phytoplankton cell size to

468   decrease in the Bering Sea as temperature increases (Fujiwara et al. 2011). Studies also report a

469   decrease in phytoplankton cell size occurs during warming, though may be mediated or driven

470   by other effects such as grazing or nutrient availability (Daufresne et al. 2009, Peter & Sommer

471   2013). The increased proportion of larger cells during the initial warm period may have been

472   related to the similar MLD and surface temperatures observed as occurred in the cold period

473   (Fig. 3A-C). However, other factors may be responsible for influencing phytoplankton

474   community structure, including nutrient availability, grazing, or shifts in seasonal phenology.

475   The reduction in cell size in the second warm period likely indicated a reduction in large size

476   diatoms that dominate the NBS phytoplankton community on average (Zhuang et al. 2014). The

477   NBS community was characterized by smaller cells in 2018 particularly on the middle shelf

478   (Fukai et al. 2020), and it also had very low proportions (~ 0.1) of large phytoplankton on the

479   middle shelf in 2014, likely due to a bloom of coccolithophores (Ladd et al. 2018). While we did

480   not measure primary production in our study, the lack of ice cover in Arctic waters has been

481   suggested to lead to increased pelagic primary production (Arrigo & van Dijken 2015), increased

482   influence of zooplankton grazing, and a reduction in material flux to the benthos thereby

483   reducing overall benthic production (Lovvorn et al. 2005). A reduction in diatoms (both pelagic

484   and sympagic) would result in reduced flux of carbon to the benthos, a situation that appears to

485   be underway in the NBS (Grebmeier 2012).

486   Redundancy analysis showed a distinction between the zooplankton community during

487   warm and cold periods. Communities from stations sampled during the cold period clustered

488   closely together, particularly on the middle shelf (Fig. 5), whereas warmer water communities

489   had a wider spread of data points (Figs. 5, 6). The copepod *Calanus* spp. and Chaetognatha

490   increased in abundance during the cold periods and were positively correlated with increased ice

491   area and negatively correlated with higher bottom temperatures (Fig. 7). Both taxa have been

492   shown to associate with Bering Shelf Water (Eisner et al. 2013, Eisner et al. 2014) and Eisner et

493   al. (2014) noted that the inner front bordered inshore by Alaska Coastal Water may be weaker

494   during cold years allowing these middle shelf species to enter onto the inner shelf. In contrast,

495   warm periods were correlated with increased abundances of two neritic Copepods > 2 mm taxa

496   (*Epilabidocera* and *Tortanus*) (Pinchuk & Eisner 2017), Copepods < 2 mm (with the exception

497   of *Acartia* spp.), and meroplankton (Fig. 7). We hypothesize that Alaska Coastal Water

498   (Danielson et al. 2017) expanded across both shelves during the warm periods bringing the

499   neritic zooplankton community with it. Eisner et al. (2020b) reported that distributions of

500   walleye pollock followed a similar pattern, with a more narrow longitudinal distribution during

501   2010 (cold year) and wide longitudinal distribution during warm years (2017-2019). The

502   increase in copepod numbers overall was likely a function of increased temperatures driving

503 increases in growth rate, egg production, and reduced development times (Hirst & Bunker 2003),

504 allowing abundances to accumulate. *Pseudocalanus* spp. has been found to be more responsive

505 to temperature than food in relation to these rates (Liu & Hopcroft 2008) and the latter warm

506 period showed much higher *Pseudocalanus* spp. abundances (Fig. 9G, H) as well as increases in

507 *Epilabidocera* (Fig8C, D), *Tortanus* (Fig. 8F), and *Centropages* (Fig. 9D).

508   The other members of the holoplankton community, aside from Chaetognatha, were less

509 correlated to environmental conditions on the middle shelf, but colder conditions were associated

510 with Amphipoda and Cnidarian on the inner shelf (Fig. 7). The amphipod *Themisto libellula* has

511 been observed to increase in abundance during cold periods (Pinchuk et al. 2013); however, we

512 did not observe an increase in this species. The two large peaks of amphipods were *Themisto*

513 *pacifica* (2016, middle shelf) and *Corophium* spp. (2013, inner shelf). Since large increases in

514 these taxa were not associated with an environmental variables, we may have simply sampled an

515 anomalous patch of these organisms during the surveys. Cnidarian abundances are consistently

516 problematic to interpret due to the destructive nature of net sampling, therefore we do not draw

517 major conclusions from these abundance estimates. More interesting was the increase in

518 meroplankton observed during the warm periods. Meroplankton may dominate the plankton at

519 times and release has been associated with the spring phytoplankton bloom in the northern

520 Bering Sea and shallower Chukchi Sea (Matsuno et al. 2011, Questel et al. 2013, Kimura et al.

521 2020). Kimura et al. (2020) found all three meroplankton groups we identified had peaked on the

522 NBS shelf inshore of 170°W during August of 2017, suggesting seasonal release of

523 meroplankton may be later in the year in the NBS and tied to ice retreat timing. For example,

524 earlier ice retreat and warmer bottom temperatures appeared to stimulate the release of Cirripedia

525 in the Chukchi Sea (Matsuno et al. 2011).

526   Shifts in the zooplankton community have impacts on higher trophic level predators often

527   through the impact on key forage taxa such as *Calanus* spp. We found *Calanus* spp. variability in

528   response to warm and cold periods to be similar to that observed over a shorter time period

529   (2003-2009) in the NBS (Eisner et al. 2014) and over the southeastern shelf (Baier & Napp 2003,

530   Coyle et al. 2008, Eisner et al. 2018, Kimmel et al. 2018) with this taxon positively correlating

531   with increased ice cover, cold pool area, and low bottom water temperatures (Fig. 7) (Eisner et

532   al. 2013, Eisner et al. 2014). Much remains to learn about *Calanus* spp. biology in this region,

533   including which specific species of *Calanus* may be present (Nelson et al. 2009) and whether

534   *Calanus* spp. diapause dynamics are changing in response to warming. We are seeing

535   preliminary evidence that a second generation of *Calanus* spp. may be present on the Bering Sea

536   shelf (Pinchuk et al. 2014) as has been shown at lower latitudes and has been predicted with life-

537   history modeling (Banas et al. 2016). Our results suggest that continued warming of the NBS

538   will result in a decline in *Calanus* spp. abundance in this region. This decline in *Calanus* spp.

539   may impact adult fish that were seen to move northwards during the low ice events of 2017/2018

540   and 2018/2019 (Stevenson & Lauth 2018, Eisner et al. 2020b) as well as juvenile fish that rely

541   on *Calanus* spp. as prey for lipid acquisition prior to overwintering (Heintz et al. 2013). We also

542   observed a large increase in abundance of the copepod *E. longipedata*, a little studied copepod

543   that may be a significant portion of juvenile pink salmon (*Oncorhynchus gorbuscha*) diets at

544   times (Armstrong et al. 2005). It remains to be seen whether this species will become more

545   prevalent in Bering Sea waters in the future.

546   The increase in smaller-sized zooplankton during the latter warm period may offer a

547   glimpse into the future Bering Sea, which is projected to continue to warm (Hermann et al.

548   2019). Size decrease is thought to be a global response in ectotherms to increasing temperature

24

549   (Gardner et al. 2011). A reduction in zooplankton size has been observed in mesocosms (Garzke

550   et al. 2015) and in long-term time-series of zooplankton (Rice et al. 2015) in response to warmer

551   temperatures. Both the body size of individuals (Miller et al. 1992) and overall, mean body size

552   of the zooplankton community (Chiba et al. 2015) have been shown to decline during warm

553   periods. A community of smaller-sized zooplankton grazing on smaller sized phytoplankton

554   would decrease trophic transfer efficiency (greater number of links in food web) and reduce the

555   delivery of ungrazed phytoplankton to the benthos (Lovvorn et al. 2016). The result would be

556   more carbon cycling in the pelagic, favoring the accumulation of small copepods. Smaller-

557   bodied zooplankton are lower in energy density and are often lipid-poor relative to larger

558   zooplankton (Siddon et al. 2013, Gorokhova 2019). The increase in smaller-sized zooplankton

559   taxa may also accompany a decline in the lipid-rich *Calanus* spp., though it has been suggested

560   that the increasing number of smaller zooplankton (with some lipid storage) may compensate for

561   the loss of lipid-rich species of *Calanus* (Renaud et al. 2018). However, we must caution against

562   over interpretation of our results as the reduced ice cover in 2017-2018 may be a single,

563   infrequent event. Nevertheless, if the reduction of ice cover across the Arctic continues as

564   predicted by some models (Peng et al. 2020), it will result in widespread ecosystem change.

565

566   5. CONCLUSIONS

567   We compared the northern Bering Sea zooplankton community across one cold and two

568   warm periods. Similar to prior studies, we found that the cold and warm periods differed in

569   zooplankton community response; however, the community response was particularly striking

570   during the 2017/2018 low ice event. The NBS zooplankton community had a weaker response to

571   the first warm period, suggesting that the persistence of ice cover in this region, even during

572   warm periods, appears to provide some buffer to broad-scale zooplankton community change.

573   However, the low ice extent experienced in 2017/2018 resulted in positive abundance anomalies

574   for small copepods, particularly on the middle shelf, which coincided with a decline in *Calanus*

575   spp. abundance. This response is similar to what has been observed in the SEBS and suggests

576   that the NBS zooplankton community will respond similarly if a particular minimum ice cover

577   extent and retreat threshold is reached. It also suggests an increased role of smaller-bodied

578   zooplankton in cycling of energy in the NBS if the open- water period increases substantially as

579   ice retreats. The result would be a transition from tight benthic-pelagic coupling to a decoupled

580   pelagic ecosystem.

581

582   6. ACKNOWLEDGEMENTS

593

594   7. LITERATURE CITED

Armstrong JL, Boldt JL, Cross AD, Moss JH, Davis ND, Myers KW, Walker RV, Beauchamp
	DA, Haldorson LJ (2005) Distribution, size, and interannual, seasonal and diel food
	habits of northern Gulf of Alaska juvenile pink salmon. Deep-Sea Research Part II:
	Topical Studies in Oceanography 52:247-265
Arrigo KR, van Dijken GL (2015) Continued increases in Arctic Ocean primary production.
	Progress in Oceanography 136:60-70
Baier CT, Napp JM (2003) Climate-induced variability in *Calanus marshallae* populations.
	Journal of Plankton Research 25:771-782
Banas NS, Møller EF, Nielsen TG, Eisner LB (2016) Copepod Life Strategy and Population
	Viability in Response to Prey Timing and Temperature: Testing a New Model across
	Latitude, Time, and the Size Spectrum. Frontiers in Marine Science 3:225
Basyuk E, Zuenko Y (2020) Extreme oceanographic conditions in the northwestern Bering Sea
	in 2017–2018. Deep-Sea Research Part II: Topical Studies in Oceanography 181-182
Baumgartner MF, Lysiak NSJ, Esch HC, Zerbini AN, Berchok CL, Clapham PJ (2013)
	Associations between North Pacific right whales and their zooplanktonic prey in the
	southeastern Bering Sea. Marine Ecology Progress Series 490:267-284
Bi H, Yu H, Pinchuk AI, Harvey HR (2015) Interannual summer variability in euphausiid
	populations on the eastern Bering Sea shelf during the recent cooling event (2008-2010).
	Deep-Sea Research Part I-Oceanographic Research Papers 95:12-19
Bond NA, Adams JM (2002) Atmospheric forcing of the southeast Bering Sea Shelf during
	1995-1999 in the context of a 40-year historical record. Deep-Sea Research II 49:5869-
	5887
Borcard D, Gillet F, Legendre P (2011) Numerical Ecology with R. Springer, New York
Boveng P (2019) Unusual Mortality Event: Ice Seals. In: Siddon E, Zador S (eds) Ecosystem
	Status Report 2019: Eastern Bering Sea, Stock Assessment and Fishery Evaluation
	Report. North Pacific Fishery Management Council, Anchorage, AK
Boveng PL, Ziel HL, McClintock BT, Cameron MF (2020) Body condition of phocid seals
	during a period of rapid environmental change in the Bering Sea and Aleutian Islands,
	Alaska. Deep-Sea Research Part II: Topical Studies in Oceanography 181-182
Buckley TW, Ortiz I, Kotwicki S, Aydin K (2016) Summer diet composition of walleye pollock
	and predator–prey relationships with copepods and euphausiids in the eastern Bering Sea,
	1987–2011. Deep-Sea Research Part II: Topical Studies in Oceanography 134:302-311
Chiba S, Batten SD, Yoshiki T, Sasaki Y, Sasaoka K, Sugisaki H, Ichikawa T (2015)
	Temperature and zooplankton size structure: climate control and basin-scale comparison
	in the North Pacific. Ecology and Evolution 5:968-978
Choquet M, Kosobokova K, Kwasniewski S, Hatlebakk M, Dhanasiri AKS, Melle W, Daase M,
	Svensen C, Soreide JE, Hoarau G (2018) Can morphology reliably distinguish between
	the copepods Calanus finmarchicus and C-glacialis, or is DNA the only way? Limnology
	and Oceanography-Methods 16:237-252
Clement Kinney J, Maslowski W, Osinski R, Lee YJ, Goethel C, Frey K, Craig A (2022) On the
	variability of the Bering Sea Cold Pool and implications for the biophysical environment.
	PLoS One 17:e0266180
Coachman LK (1986) Circulation, water masses, and fluxes on the southeastern Bering Sea
	shelf Bering Sea shelf. Continental Shelf Research 5:23-108
Coachman LK, Aagaard K, Tripp RB (1975) Bering Strait: The Regional Physical
	Oceanography. University of Washington Press, Seattle, Washington, USA

Cooney RT, Coyle KO (1982) Trophic implication of cross-shelf copepod distributions in the southeastern Bering Sea. Marine Biology 70:187-196

Coyle KO, Gibson GA (2017) *Calanus* on the Bering Sea shelf: probable cause for population declines during warm years. Journal Of Plankton Research 39:257-270

Coyle KO, Pinchuk AI (2002) Climate-related differences in zooplankton density and growth on the inner shelf of the southeastern Bering Sea. Progress in Oceanography 55:177-194

Coyle KO, Pinchuk AI, Eisner LB, Napp JM (2008) Zooplankton species composition, abundance and biomass on the eastern Bering Sea shelf during summer: The potential role of water-column stability and nutrients in structuring the zooplankton community. Deep-Sea Research Part II-Topical Studies in Oceanography 55:1775-1791

Danielson S, Eisner L, Weingartner T, Aagaard K (2011) Thermal and haline variability over the central Bering Sea shelf: Seasonal and interannual perspectives. Continental Shelf Research 31:539-554

Danielson S, Hedstrom K, Aagaard K, Weingartner T, Curchitser E (2012) Wind-induced reorganization of the Bering shelf circulation. Geophysical Research Letters 39:1-6

Danielson SL, Ahkinga O, Ashjian C, Basyuk E, Cooper LW, Eisner L, Farley E, Iken KB, Grebmeier JM, Juranek L, Khen G, Jayne SR, Kikuchi T, Ladd C, Lu K, McCabe RM, Moore GWK, Nishino S, Ozenna F, Pickart RS, Polyakov I, Stabeno PJ, Thoman R, Williams WJ, Wood K, Weingartner TJ (2020) Manifestation and consequences of warming and altered heat fluxes over the Bering and Chukchi Sea continental shelves. Deep-Sea Research Part II: Topical Studies in Oceanography

Danielson SL, Eisner L, Ladd C, Mordy C, Sousa L, Weingartner TJ (2017) A comparison between late summer 2012 and 2013 water masses, macronutrients, and phytoplankton standing crops in the northern Bering and Chukchi Seas. Deep-Sea Research Part II: Topical Studies in Oceanography 135:7-26

Daufresne M, Lengfellner K, Sommer U (2009) Global warming benefits the small in aquatic ecosystems. Proceedings of the National Academy of Sciences of the United States of America 106:12788-12793

Dinno A (2017) dunn.test: Dunn's Test of Multiple Comparisons Using Rank Sums. R package version 135 https://CRAN.R-project.org/package=dunn.test

Duffy-Anderson JT, Stabeno P, Andrews AG, Cieciel K, Deary A, Farley E, Fugate C, Harpold C, Heintz R, Kimmel D, Kuletz K, Lamb J, Paquin M, Porter S, Rogers L, Spear A, Yasumiishi E (2019) Responses of the northern Bering Sea and southeastern Bering Sea pelagic ecosystems following record-breaking low winter sea ice. Geophysical Research Letters 46:9833-9842

Duffy-Anderson JT, Stabeno PJ, Siddon EC, Andrews AG, Cooper DW, Eisner LB, Farley EV, Harpold CE, Heintz RA, Kimmel DG, Sewall FF, Spear AH, Yasumishii EC (2017) Return of warm conditions in the southeastern Bering Sea: Phytoplankton - Fish. PLoS One 12:e0178955

Dunn OJ (1964) Multiple comparisons using rank sums. Technometrics 6:241-252

Eisner L, Cieciel K, Gann J, Ladd C (2019) Phytoplankton biomass and size structure during late summer to early fall in the eastern Bering Sea. In: Zador S, Siddon E (eds) Ecosystem Status Report 2019: Eastern Bering Sea. North Pacific Fishery Management Council, 1007 West Third, Suite 400, Anchorage, AK 99501

685 Eisner L, Hillgruber N, Martinson E, Maselko J (2013) Pelagic fish and zooplankton species
686   assemblages in relation to water mass characteristics in the northern Bering and southeast
687   Chukchi seas. Polar Biology 36:87-113
688 Eisner LB, Napp JM, Mier KL, Pinchuk AI, Andrews AG, III (2014) Climate-mediated changes
689   in zooplankton community structure for the eastern Bering Sea. Deep-Sea Research Part
690   II-Topical Studies in Oceanography 109:157-171
691 Eisner LB, Pinchuk AI, Kimmel DG, Mier KL, Harpold CE, Siddon EC, Hidalgo M (2018)
692   Seasonal, interannual, and spatial patterns of community composition over the eastern
693   Bering Sea shelf in cold years. Part I: zooplankton. ICES Journal of Marine Science
694   75:72-86
695 Eisner LB, Yasumiishi EM, Andrews III AG, O'Leary C (2020a) Large copepods as leading
696   indicators of walleye pollock recruitment in the southeastern Bering Sea: Sample-based
697   and spatio-temporal model (VAST) results. Fisheries Research 232:105720
698 Eisner LB, Zuenko YI, Basyuk EO, Britt LL, Duffy-Anderson JT, Kotwicki S, Ladd C, Cheng W
699   (2020b) Environmental impacts on walleye pollock (*Gadus chalcogrammus*) distribution
700   across the Bering Sea shelf. Deep-Sea Research Part II: Topical Studies in Oceanography
701   181-182
702 Ershova EA, Hopcroft RR, Kosobokova KN (2015) Inter-annual variability of summer
703   mesozooplankton communities of the western Chukchi Sea: 2004-2012. Polar Biology
704   38:1461-1481
705 Fedewa EJ, Jackson TM, Richar JI, Gardner JL, Litzow MA (2020) Recent shifts in northern
706   Bering Sea snow crab (*Chionoecetes opilio*) size structure and the potential role of
707   climate-mediated range contraction. Deep Sea Research Part II: Topical Studies in
708   Oceanography 181-182
709 Fox J, Weisberg S (2019) An R companion to Applied Regression. Sage Publications, Thousand
710   Oaks, California
711 Frost BW (1974) *Calanus marshallae*, a new species of calanoid copepod closely allied to the
712   sibling species *C. finmarchicus* and *C. glacialis*. Marine Biology 26:77-99
713 Fujiwara A, Hirawake T, Suzuki K, Saitoh SI (2011) Remote sensing of size structure of
714   phytoplankton communities using optical properties of the Chukchi and Bering Sea shelf
715   region. Biogeosciences 8:3567-3580
716 Fukai Y, Abe Y, Matsuno K, Yamaguchi A (2020) Spatial changes in the summer diatom
717   community of the northern Bering Sea in 2017 and 2018. Deep-Sea Research Part Ii-
718   Topical Studies in Oceanography 181
719 Gardner JL, Peters A, Kearney MR, Joseph L, Heinsohn R (2011) Declining body size: a third
720   universal response to warming? Trends in Ecology & Evolution 26:285-291
721 Garzke J, Ismar SMH, Sommer U (2015) Climate change affects low trophic level marine
722   consumers: warming decreases copepod size and abundance. Oecologia 177:849-860
723 Gorbatenko KM, Dolganova NT (2007) Comparing the catch efficiency with different types of
724   plankton nets in the high production zones of the Pacific Ocean. Oceanology 47:205-212
725 Gorokhova E (2019) Individual body size as a predictor of lipid storage in Baltic Sea
726   zooplankton. Journal of Plankton Research 41:273-280
727 Grebmeier JM (2012) Shifting Patterns of Life in the Pacific Arctic and Sub-Arctic Seas. In:
728   Carlson CA, Giovannoni SJ (eds) Annual Review of Marine Science, Vol 4, Book 4
729 Heintz RA, Siddon EC, Farley EV, Napp JM (2013) Correlation between recruitment and fall
730   condition of age-0 pollock (*Theragra chalcogramma*) from the eastern Bering Sea under

varying climate conditions. Deep-Sea Research Part II-Topical Studies in Oceanography 94:150-156

Hermann AJ, Gibson GA, Bond NA, Curchitser EN, Hedstrom K, Cheng W, Wang M, Cokelet ED, Stabeno PJ, Aydin K (2016) Projected future biophysical states of the Bering Sea. Deep-Sea Research II 134:30-47

Hermann AJ, Gibson GA, Cheng W, Ortiz I, Aydin K, Wang M, Hollowed AB, Holsman KK, Sathyendranath S (2019) Projected biophysical conditions of the Bering Sea to 2100 under multiple emission scenarios. ICES Journal of Marine Science 76:1280-1304

Hirst AG, Bunker AJ (2003) Growth of marine planktonic copepods: global rates and patterns in relation to chlorophyll *a*, temperature, and body weight. Limnology and Oceanography 48:1988-2010

Hopcroft RR, Kosobokova KN, Pinchuk AI (2010) Zooplankton community patterns in the Chukchi Sea during summer 2004. Deep-Sea Research Part II-Topical Studies in Oceanography 57:27-39

Hunt GL, Coyle KO, Eisner LB, Farley EV, Heintz RA, Mueter F, Napp JM, Overland JE, Ressler PH, Salo S, Stabeno PJ (2011) Climate impacts on eastern Bering Sea foodwebs: a synthesis of new data and an assessment of the Oscillating Control Hypothesis. ICES Journal of Marine Science 68:1230-1243

Hunt GL, Ressler PH, Gibson GA, De Robertis A, Aydin K, Sigler MF, Ortiz I, Lessard EJ, Williams BC, Pinchuk A, Buckley T (2016) Euphausiids in the eastern Bering Sea: A synthesis of recent studies of euphausiid production, consumption and population control. Deep-Sea Research Part II: Topical Studies in Oceanography 134:204-222

Jones MC, Berkelhammer M, Keller KJ, Yoshimura K, Wooller MJ (2020) High sensitivity of Bering Sea winter sea ice to winter insolation and carbon dioxide over the last 5500 years. Science Advances 6:eaaz9588

Kikuchi G, Abe H, Hirawake T, Sampei M (2020) Distinctive spring phytoplankton bloom in the Bering Strait in 2018: A year of historically minimum sea ice extent. Deep-Sea Research Part II: Topical Studies in Oceanography 181-182

Kim J-H, Cho K-H, La HS, Choy EJ, Matsuno K, Kang S-H, Kim W, Yang EJ (2020) Mass occurrence of Pacific copepods in the southern Chukchi Sea during summer: Implications of the high-temperature Bering Summer water. Frontiers in Marine Science 7:612

Kimmel DG, Eisner LB, Wilson MT, Duffy-Anderson JT (2018) Copepod dynamics across warm and cold periods in the eastern Bering Sea: Implications for walleye pollock (*Gadus chalcogrammus*) and the Oscillating Control Hypothesis. Fisheries Oceanography 27:143-158

Kimura F, Abe Y, Matsuno K, Hopcroft RR, Yamaguchi A (2020) Seasonal changes in the zooplankton community and population structure in the northern Bering Sea from June to September, 2017. Deep-Sea Research Part Ii-Topical Studies in Oceanography 181

Kruskal WH, Wallis WA (1952) Use of ranks in one-criterion variance analysis. Journal of the American Statistical Association 47:583-621

Ladd C, Eisner LB, Salo SA, Mordy CW, Iglesias-Rodriguez MD (2018) Spatial and temporal variability of coccolithophore blooms in the eastern Bering Sea. Journal of Geophysical Research: Oceans 123:9119-9136

Ladd C, Stabeno PJ (2012) Stratification on the Eastern Bering Sea shelf revisited. Deep-Sea Research II 65:72-83

Levene H (1965) Robust tests for equality of variances. In: Olkin I, Ghurye SG, Hoeffding W, Madow WG, Mann HB (eds) Contributions to Probability and Statistics. Stanford University Press, Stanford, California, USA

Liu H, Hopcroft RR (2008) Growth and development of *Pseudocalanus* spp. in the northern Gulf of Alaska. Journal of Plankton Research 30:923-935

Lovvorn JR, Cooper LW, Brooks ML, De Ruyck CC, Bump JK, Grebmeier JM (2005) Organic matter pathways to zooplankton and benthos under pack ice in late winter and open water in late summer in the north-central Bering Sea. Marine Ecology Progress Series 291:135-150

Lovvorn JR, North CA, Kolts JM, Grebmeier JM, Cooper LW, Cui X (2016) Projecting the effects of climate-driven changes in organic matter supply on benthic food webs in the northern Bering Sea. Marine Ecology Progress Series 548:11-30

Matsuno K, Yamaguchi A, Hirawake T, Imai I (2011) Year-to-year changes of the mesozooplankton community in the Chukchi Sea during summers of 1991, 1992 and 2007, 2008. Polar Biology 34:1349-1360

Miller CB, Fulton J, Frost BW (1992) Size variation of *Neocalanus plumchrus* and *Neocalanus flemingeri* in a 20-yr sample series from the Gulf of Alaska. Canadian Journal of Fisheries and Aquatic Sciences 49:389-399

Nelson RJ, Carmack EC, McLaughlin FA, Cooper GA (2009) Penetration of Pacific zooplankton into the western Arctic Ocean tracked with molecular population genetics. Marine Ecology Progress Series 381:129-138

Nielsen JM, Eisner L, Watson J, Gann JC, Mordy CW, Bell SW, Harpold C, Crouser D, Stabeno P (2020) Spring satellite chlorophyll-a concentrations in the eastern Bering Sea. In: Siddon E (ed) Ecosystem Status Report 2020: Eastern Bering Sea. North Pacific Fishery Management Council, 1007 West Third, Suite 400, Anchorage, AK 99501

Oksanen J, Blanchet FG, Friendly M, Kindt R, Legendre P, McGlinn D, Minchin PR, O'Hara RB, Simpson GL, Solymos P, Stevens MHH, Szoecs E, Wanger H (2019) vegan: Community Ecology Package. R package version 25-6 https://CRAN.R-project/org/package=vegan

Ortiz I, Weise F, Grieg A (2012) Marine regions boundary data for the Bering Sea shelf and slope, version 1.0. UCAR/NCAR - Earth Observing Laboratory

Parsons TR, Maita Y, Lalli CM (1984) A Manual of Chemical and Biological Methods for Seawater Analysis. Pergamon Press, Oxford, United Kingdom

Peng G, Matthews JL, Wang M, Vose R, Sun L (2020) What Do Global Climate Models Tell Us about Future Arctic Sea Ice Coverage Changes? Climate 8

Peter KH, Sommer U (2013) Phytoplankton cell size reduction in response to warming mediated by nutrient limitation. Plos One 8

Piatt JF, Spring AM (2003) Advection, pelagic food webs and the biogeography of seabirds in Beringia. Marine Ornithology 31:141-154

Pinchuk AI, Coyle KO, Eisner LB, Napp JM (2014) Climate-induced variability in Calanus spp. development and spawning in the eastern Bering Sea. Ocean Sciences Meeting, Honolulu, Hawaii, USA

Pinchuk AI, Coyle KO, Farley EV, Renner HM (2013) Emergence of the Arctic *Themisto libellula* (Amphipoda: Hyperiidae) on the southeastern Bering Sea shelf as a result of the recent cooling, and its potential impact on the pelagic food web. ICES Journal of Marine Science 70:1244-1254

Pinchuk AI, Eisner LB (2017) Spatial heterogeneity in zooplankton summer distribution in the eastern Chukchi Sea in 2012–2013 as a result of large-scale interactions of water masses. Deep-Sea Research Part II: Topical Studies in Oceanography 135:27-39

Questel JM, Clarke C, Hopcroft RR (2013) Seasonal and interannual variation in the planktonic communities of the northeastern Chukchi Sea during the summer and early fall. Continental Shelf Research 67:23-41

R Core Team (2019) R: A language and environment for statistical computing. R Foundation for Statistical Computing, Vienna, Austria

Renaud PE, Daase M, Banas NS, Gabrielsen TM, Søreide JE, Varpe Ø, Cottier F, Falk-Petersen S, Halsband C, Vogedes D, Heggland K, Berge J (2018) Pelagic food-webs in a changing Arctic: a trait-based perspective suggests a mode of resilience. ICES Journal of Marine Science 75:1871-1881

Ressler PH, De Robertis A, Kotwicki S (2014) The spatial distribution of euphausiids and walleye pollock in the eastern Bering Sea does not imply top-down control by predation. Marine Ecology Progress Series 503:111-122

Rice E, Dam HG, Stewart G (2015) Impact of climate change on estuarine zooplankton: surface water warming in Long Island Sound is sssociated with changes in copepod size and community structure. Estuaries and Coasts 38:13-23

Richardson AJ (2008) In hot water: zooplankton and climate change. ICES Journal of Marine Science 65:279-295

Romano MD, Renner HM, Kuletz KJ, Parrish JK, Jones T, Burgess HK, Cushing DA, Causey D (2020) Die–offs, reproductive failure, and changing at–sea abundance of murres in the Bering and Chukchi Seas in 2018. Deep-Sea Research Part II: Topical Studies in Oceanography 181-182

Sameoto D, Cochrane N, Herman A (1993) Convergence of acoustic, optical, and net-catch estimates of euphausiid abundance: use of artificial light to reduce net avoidance. Canadian Journal of Fisheries and Aquatic Sciences 50:334-346

Shapiro SS, Wilk MB (1965) An analysis of variance test for normality (complete samples). Biometrika 52:591-611

Shevelev MS (2004) Study of Ecosystems of Fishery Water Bodies, Collection and Processing of Data on Aquatic Biological Resources, Equipment and Technology of Their Catch and Processing, Vol 1. VNIRO Press, Moscow, Russia

Siddon EC, Kristiansen T, Mueter FJ, Holsman KK, Heintz RA, Farley EV (2013) Spatial match-mismatch between juvenile fish and prey provides a mechanism for recruitment variability across contrasting climate conditions in the eastern Bering Sea. PLoS One 8

Siddon EC, Zador SG, Hunt GL (2020) Ecological responses to climate perturbations and minimal sea ice in the northern Bering Sea. Deep-Sea Research Part Ii-Topical Studies in Oceanography 181

Sigler MF, Stabeno PJ, Eisner LB, Napp JM, Mueter FJ (2014) Spring and fall phytoplankton blooms in a productive subarctic ecosystem, the eastern Bering Sea, during 1995-2011. Deep-Sea Research Part II-Topical Studies in Oceanography 109:71-83

Skjoldal HR, Prokopchuk I, Bagøien E, Dalpadado P, Nesterova V, Rønning J, Knutsen T (2019) Comparison of Juday and WP2 nets used in joint Norwegian–Russian monitoring of zooplankton in the Barents Sea. Journal of Plankton Research 41:759-769

Springer AM, McRoy PC, Flint MV (1996) The Bering Sea green belt: shelf-edge processes and ecosystem production. Fisheries Oceanography 5

Stabeno PJ, Bell SW (2019) Extreme conditions in the Bering Sea (2017–2018): record-breaking low sea-ice extent. Geophysical Research Letters 46:8952-8959

Stabeno PJ, Bell SW, Bond NA, Kimmel DG, Mordy CW, Sullivan ME (2019) Distributed Biological Observatory Region 1: Physics, chemistry and plankton in the northern Bering Sea. Deep-Sea Research Part II: Topical Studies in Oceanography 162:8-21

Stabeno PJ, Bond NA, Kachel NB, Salo SA, Schumacher JD (2001) On the temporal variablity of the physical environment over the southeastern Bering Sea. Fisheries Oceanography 10:81-98

Stabeno PJ, Farley EV, Jr., Kachel NB, Moore S, Mordy CW, Napp JM, Overland JE, Pinchuk AI, Sigler MF (2012a) A comparison of the physics of the northern and southern shelves of the eastern Bering Sea and some implications for the ecosystem. Deep-Sea Research Part II-Topical Studies in Oceanography 65-70:14-30

Stabeno PJ, Kachel NB, Moore SE, Napp JM, Sigler M, Yamaguchi A, Zerbini AN (2012b) Comparison of warm and cold years on the southeastern Bering Sea shelf and some implications for the ecosystem. Deep-Sea Research Part II-Topical Studies in Oceanography 65-70:31-45

Stevenson DE, Lauth RR (2018) Bottom trawl surveys in the northern Bering Sea indicate recent shifts in the distribution of marine species. Polar Biology 42:407-421

Strasburger WW, Hillgruber N, Pinchuk AI, Mueter FJ (2014) Feeding ecology of age-0 walleye pollock (*Gadus chalcogrammus*) and Pacific cod (*Gadus macrocephalus*) in the southeastern Bering Sea. Deep-Sea Research Part II: Topical Studies in Oceanography 109:172-180

Stroeve J, Meier WN (2018) Sea Ice Trends and Climatologies from SMMR and SSM/I-SSMIS, Version 3. NASA National Snow and Ice Data Center Distributed Active Archive Center, Boulder, CO

Tarrant AM, Eisner LB, Kimmel DG (2021) Lipid-related gene expression and sensitivity to starvation in Calanus glacialis in the eastern Bering Sea. Marine Ecology Progress Series 674:73-88

Thoman RL, Bhatt US, Bieniek PA, Brettschneider BR, Brubaker M, Danielson SL, Labe Z, Lader R, Meier WN, Sheffield G, Walsh JE (2020) The Record Low Bering Sea Ice Extent in 2018: Context, Impacts, and an Assessment of the Role of Anthropogenic Climate Change. Bulletin of the American Meteorological Society 101:S53-S58

Thompson DWJ, Wallace JM (1998) The Arctic Oscillation signature in the wintertime geopotential hieght and temperature fields. Geophysical Research Letters 25:1297-1300

Thorson JT, Adams CF, Brooks EN, Eisner LB, Kimmel DG, Legault CM, Rogers LA, Yasumiishi EM, Siddeek MSM (2020) Seasonal and interannual variation in spatio-temporal models for index standardization and phenology studies. ICES Journal of Marine Science 77:1879-1892

Trenberth KE, Hurrell JW (1994) Decadal atmosphere-ocean variations in the Pacific. Climate Dynamics 9:303-319

Tukey J (1949) Comparing Individual Means in the Analysis of Variance. Biometrics 5:99-114

Ueno H, Komatsu M, Ji ZQY, Dobashi R, Muramatsu M, Abe H, Imai K, Ooki A, Hirawake T (2020) Stratification in the northern Bering Sea in early summer of 2017 and 2018. Deep-Sea Research Part Ii-Topical Studies in Oceanography 181

912   Vidal J, Smith SL (1986) Biomass, growth, and development of populations of herbivorous
913   zooplankton in the southeastern Bering Sea during spring. Deep-Sea Research Part a-
914   Oceanographic Research Papers 33:523-556
915   Will A, Takahashi A, Thiebot JB, Martinez A, Kitaiskaia E, Britt L, Nichol D, Murphy J,
916   Dimond A, Tsukamoto S, Nishizawa B, Niizuma Y, Kitaysky A (2020) The breeding
917   seabird community reveals that recent sea ice loss in the Pacific Arctic does not benefit
918   piscivores and is detrimental to planktivores. Deep-Sea Research Part II-Topical Studies
919   in Oceanography 181
920   Yamaguchi A, Kimura F, Fukai Y, Abe Y, Matsuno K, Ooki A, Hirawake T (2021) Between-
921   year comparison of interactions between environmental parameters and various plankton
922   stocks in the northern Bering Sea during the summers of 2017 and 2018. Polar Science 27
923   Yasumiishi EM, Cieciel K, Andrews AG, Murphy J, Dimond JA (2020) Climate-related changes
924   in the biomass and distribution of small pelagic fishes in the eastern Bering Sea during
925   late summer, 2002–2018. Deep-Sea Research Part II: Topical Studies in Oceanography
926   181-182
927   Zhuang YP, Jin HY, Li HL, Chen JF, Wang B, Chen FJ, Bai YC, Lu Y, Tian SC (2014)
928   Phytoplankton composition and its ecological effect in subsurface cold pool of the
929   northern Bering Sea in summer as revealed by HPLC derived pigment signatures. Acta
930   Oceanologica Sinica 33:103-111

931

932 TABLES

933

934 Table 1. Climate and environmental variables used to calculate standardized anomalies and conduct the redundancy analysis for the

935 survey period 2002-2018, including abbreviation, source, reference, and hyperlink.

936

Variable	Abbreviation	Source	Reference	Link
Arctic Oscillation Nov-Mar Mean Index	AO	NWS CPC[1]	Thompson and Wallace (1998)	https://www.cpc.ncep.noaa.gov/products/precip/CWlink/daily_ao_index/ao_index.html
North Pacific Index Nov-Mar Mean Index	NPI	NCAR[2]	Trenberth and Hurrell (1994)	https://climatedataguide.ucar.edu/sites/default/files/npindex_anom_ndjfm.txt
Ice area anomaly (Jan-Apr) (km^2)	IA	NASA NSIDC[3]	Stroeve and Meier (2018)	https://nsidc.org/
Ice percentage around M8 mooring in March	M8I	NASA NSIDC[3]	Stroeve and Meier (2018)	https://nsidc.org/
Summer cold pool extent (km^2)	CP	NMFS bottom trawl survey[4]	Fedewa et al. (2020)	https://www.fisheries.noaa.gov/alaska/commercial-fishing/alaska-groundfish-bottom-trawl-survey-data
Wind mixing Jun-Sep (Summer) ($m\ s^{-1}$)	WM	NCEP/NCAR Reanalysis[5]	Danielson et al. (2012)	http://apdrc.soest.hawaii.edu/erddap/griddap

SE wind Feb-May (Spring) (m s⁻¹)	SpSE	NCEP/NCAR Reanalysis[5]	Danielson et al. (2012)	http://apdrc.soest.hawaii.edu/erddap/griddap
SE wind Jun-Sep (Summer) (m s⁻¹)	SuSE	NCEP/NCAR Reanalysis[5]	Danielson et al. (2012)	http://apdrc.soest.hawaii.edu/erddap/griddap
NW wind Feb-May (Spring) (m s⁻¹)	SpNW	NCEP/NCAR Reanalysis[5]	Danielson et al. (2012)	http://apdrc.soest.hawaii.edu/erddap/griddap
NW wind Jun-Sep (Summer) (m s⁻¹)	SuNW	NCEP/NCAR Reanalysis[5]	Danielson et al. (2012)	http://apdrc.soest.hawaii.edu/erddap/griddap
Mixed layer depth (m)	MLD	CTD		
Surface temperature (°C)	ST	CTD		
Bottom temperature (°C)	BT	CTD		
Surface salinity	SS	CTD		
Bottom salinity	BS	CTD		
Total Chl a (µg L⁻¹)	TC	Bottle samples		
Chl a > 10 µm (µg L⁻¹)	CG10	Bottle samples		

937 [1]National Weather Service, Climate Prediction Center, [2]National Center for Atmospheric Research, [3]National Aeronautics and Space

938 Administration, National Snow and Ice Data Center, [4]National Marine Fisheries Service, [5]National Center for Environmental

939 Prediction/National Center for Atmospheric Research

940

Table 2. Zooplankton data collection: year of survey, total number of net tows for each gear type: 37 cm diameter, 168 µm mesh net (Juday); 20 cm diameter, 153 µm mesh bongo net (20 cm); 60 cm diameter, 505 µm mesh ring or bongo net (60 cm) within the middle and inner shelf regions, and dates when the surveys were conducted.

Year	Juday (N)		20 cm (N)		60 cm (N)		Dates
	Inner	Middle	Inner	Middle	Inner	Middle	
2002					14	10	17-24 Sep
2003	7	4			16	8	28 Sep – 2 Oct
2004	7	11			16	19	14-28 Sep
2005	7	9		2	16	16	17 Sep - 4 Oct
2006	6	8		11	15	14	4 Sep – 10 Oct
2007	7	8		17	13	12	17 Sep – 11 Oct
2008							
2009	13	13	1	18	13	12	1 Sep – 11 Oct
2010	16	8			9	3	14-25 Sep
2011	18	8		1	16	7	24 Aug – 25 Sep
2012			13	1	13		29 Aug - 28 Sep
2013					11	3	17-24 Sep
2014			16	27	16	26	14-24 Sep
2015			15	17	15	17	1 Sep – 6 Oct
2016			16	10	16	10	28 Aug – 18 Sep
2017			17	17	17	17	28 Aug – 9 Sep
2018			16	8	17	8	1-10 Sep

945   Table 3. Taxa considered in the multivariate analysis, abbreviation, gear type: 37 cm diameter,

946   168 μm mesh net (Juday); 20 cm diameter, 153 μm mesh bongo net (20 cm); 60 cm diameter,

947   505 μm mesh ring or bongo net (60 cm), zooplankton stage or size limit, and group. For

948   copepods, C refers to copepodite and the number to stage, with 6 being the adult stage.

949

Taxa	Abbreviation	Gear	Stage/Size	Group
Calanus spp.	CA	20 cm/60 cm	C3-C6	Copepods > 2 mm
Epilabidocera longipedata	EP	20 cm/60 cm	C1-C6	Copepods > 2 mm
Tortanus discaudatus	TO	20 cm/60 cm	C1-C6	Copepods > 2 mm
Acartia spp.	AC	Juday/20 cm	C1-C6	Copepods < 2 mm
Centropages abdominalis	CE	20 cm/60 cm	C1-C6	Copepods < 2 mm
Oithona spp.	OI	Juday/20 cm	C1-C6	Copepods < 2 mm
Pseudocalanus spp.	PS	Juday/20 cm	C1-C6	Copepods < 2 mm
Amphipoda	AM	60 cm	< 20 mm	Other Holoplankton
Appendicularia	AP	60 cm	< 20 mm	Other Holoplankton
Chaetognatha	CH	60 cm	< 20 mm	Other Holoplankton
Cnidaria	CN	60 cm	Medusa	Other Holoplankton
Limacina helicina	LH	60 cm	< 20 mm	Other Holoplankton
Bivalvia	BI	Juday/20 cm	Larvae	Meroplankton
Cirripedia	CI	60 cm	Nauplius/Cypris	Meroplankton
Polychaeta	PO	Juday/20 cm	Larvae	Meroplankton

950

951

952 Table 4. Step-wise model selection results for the middle and inner shelf zooplankton community
953 redundancy analyses: Columns show variables included in each iteration of the model selection,
954 as well as the corresponding Akaike Information Criterion (AIC) values, F values, and p-values.
955 The r^2 value represents the result for the full model. Variable abbreviations can be found in
956 Table 1.

957

Variable	Middle Shelf ($r^2 = 0.34$)		
	AIC	F	p
IA + TC + CG10 + CP + M8I + BT	-50.79	2.28	0.01
IA + TC + CG10 + CP + M8I	-50.25	2.12	0.03
IA + TC + CG10 + CP	-49.93	2.65	0.01
IA + TC + CG10	-49.09	2.83	0.005
IA + TC	-48.13	3.49	0.005
IA	-46.86	4.57	0.005
	Inner shelf ($r^2 = 0.26$)		
M8I + BT + IA + CP	-67.79	2.65	0.005
M8I + BT + IA	-67.001	3.34	0.005
M8I + BT	-65.55	5.03	0.005
M8I	-62.49	5.41	0.005

958
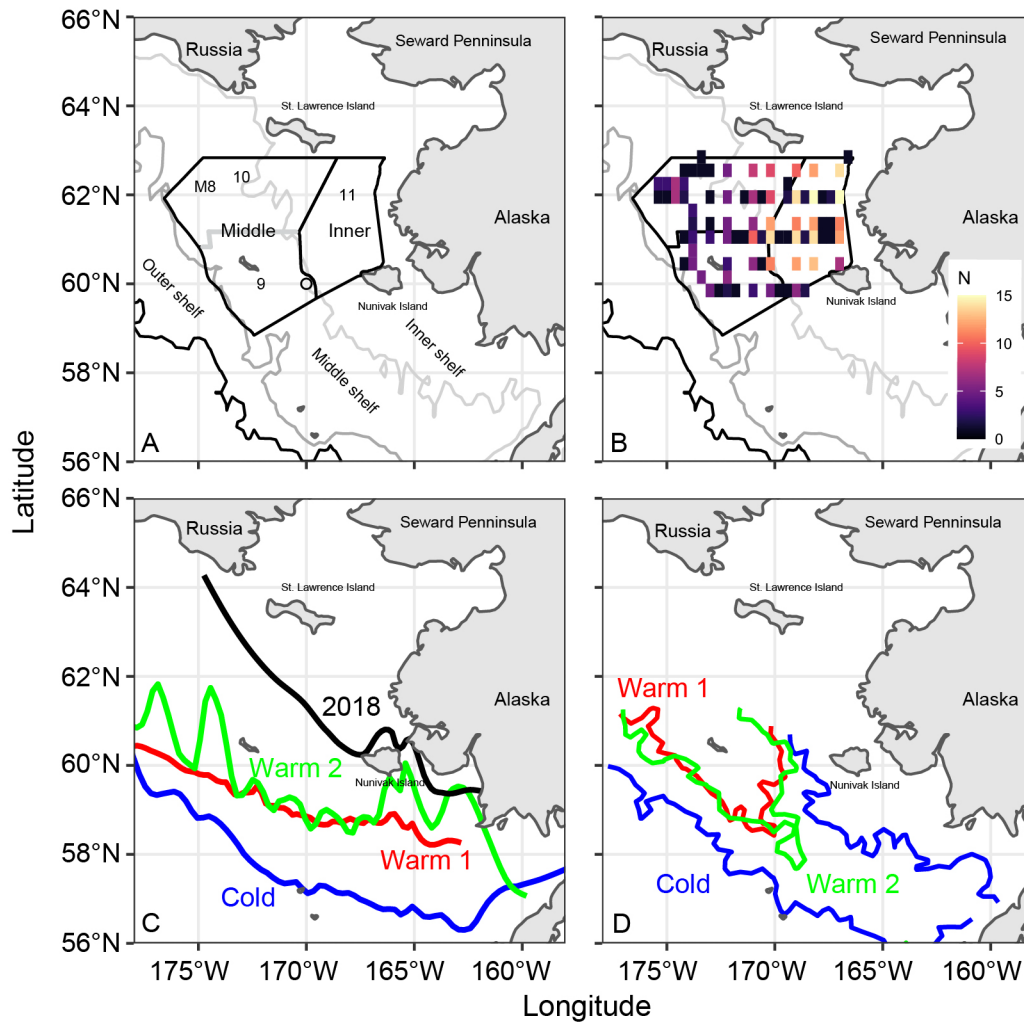
Figure 1. Map of the study area showing the North Middle Shelf (Middle; combined areas of Ortiz et al. 2012 regions 9 and 10) and the North Inner Shelf (Inner; Ortiz et al. 2012 region 11) regions (A). Location of the M8 mooring site is indicated and the closed circle represents the location used for wind data (60°N, 170°W) (A). Light gray line represents the 50 m isobath, dark gray line represents the 100 m isobath, and solid black line to the west represents the 200 m isobath and these isobaths are used as separators for the inner, middle, and outer shelf respectively (A). Sample count (N) for the entire study period (B). Average ice-extent as of 15 March (C) and average location of the 2°C bottom temperature isotherm, indicator of the cold pool extent (D) for warm period 1 (Warm 1 2003-2005; red), cold period (Cold 2006-2013; blue), and warm period 2 (Warm 2 2014-2018; green). Also shown is ice extent in 2018, a year of record low ice cover in the Bering (C, black). The cold pool was not detected within the survey boundary in 2018.

974
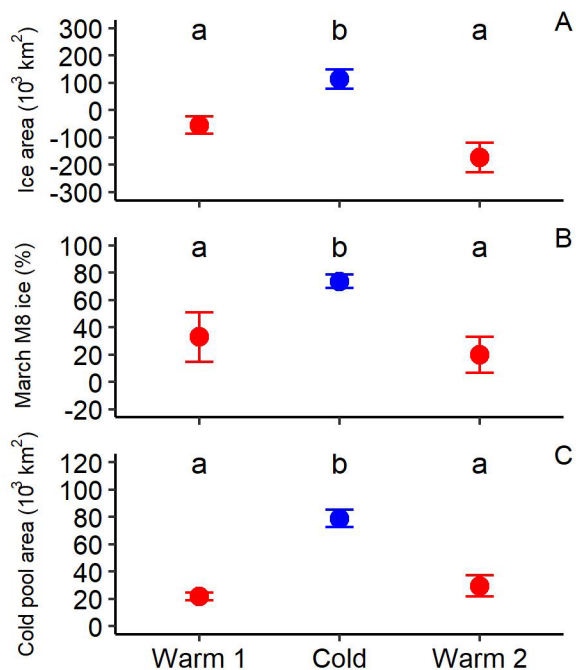
Figure 2. Comparisons of total ice area (A), March percent ice cover around M8 mooring (B), and cold pool area (C) across Warm 1 (2002-2005, red), Warm 2 (2014-2018, red) and cold (2006-2013, blue) periods. Points represent time-period mean and error bars $\pm$ 1 SE of the mean (Warm 1 $N = 4$, Cold $N = 8$, Warm 2 $N = 5$). Periods that have different lower case letters had means that differed based on one-way ANOVA ($p < 0.05$) and Tukey Honest Significant Differences *post-hoc* tests ($p < 0.05$) and periods with the same lower case letter did not.

981
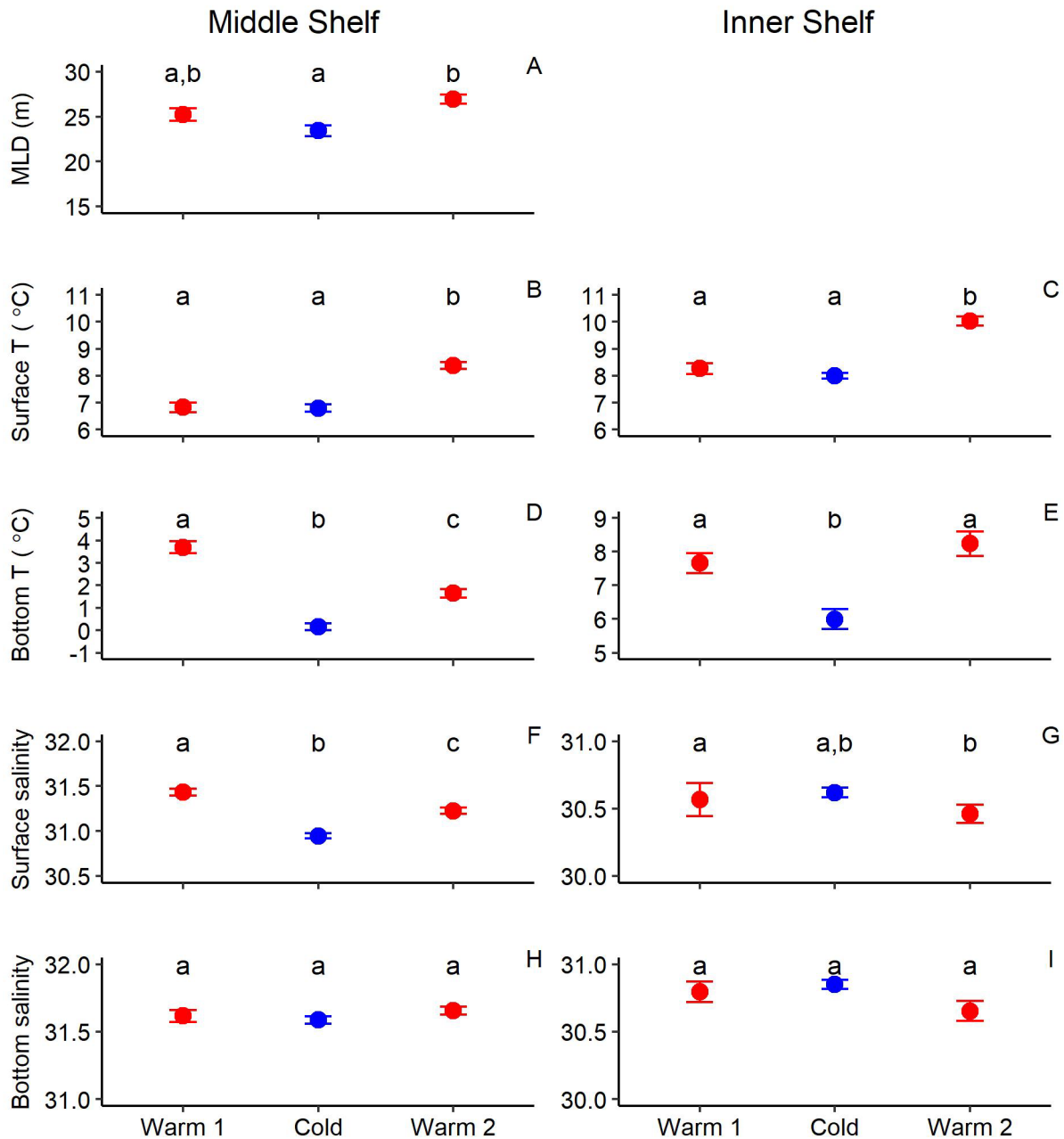
Figure 3. Comparisons of mixed layer depth (MLD) (A), surface temperature (B, C), bottom temperature (D, E), surface salinity (F, G), and bottom salinity (H, I) across Warm 1 (2002-2005, red), Warm 2 (2014-2018, red) and Cold (2006-2013, blue) periods for the middle (left panels) and inner shelf (right panels). Points represent time-period mean and error bars ± 1 SE of the mean (Middle: Warm 1 $N = 67$, Cold $N = 108$, Warm 2 $N = 140$; Inner: Warm 1 $N = 63$, Cold $N = 110$, Warm 2 $N = 81$). Periods that have different lower case letters had means that differed based on Kruskal-Wallis ($p < 0.05$) and Dunn's *post-hoc* tests ($p < 0.05$) and periods with the same lower case letter did not.
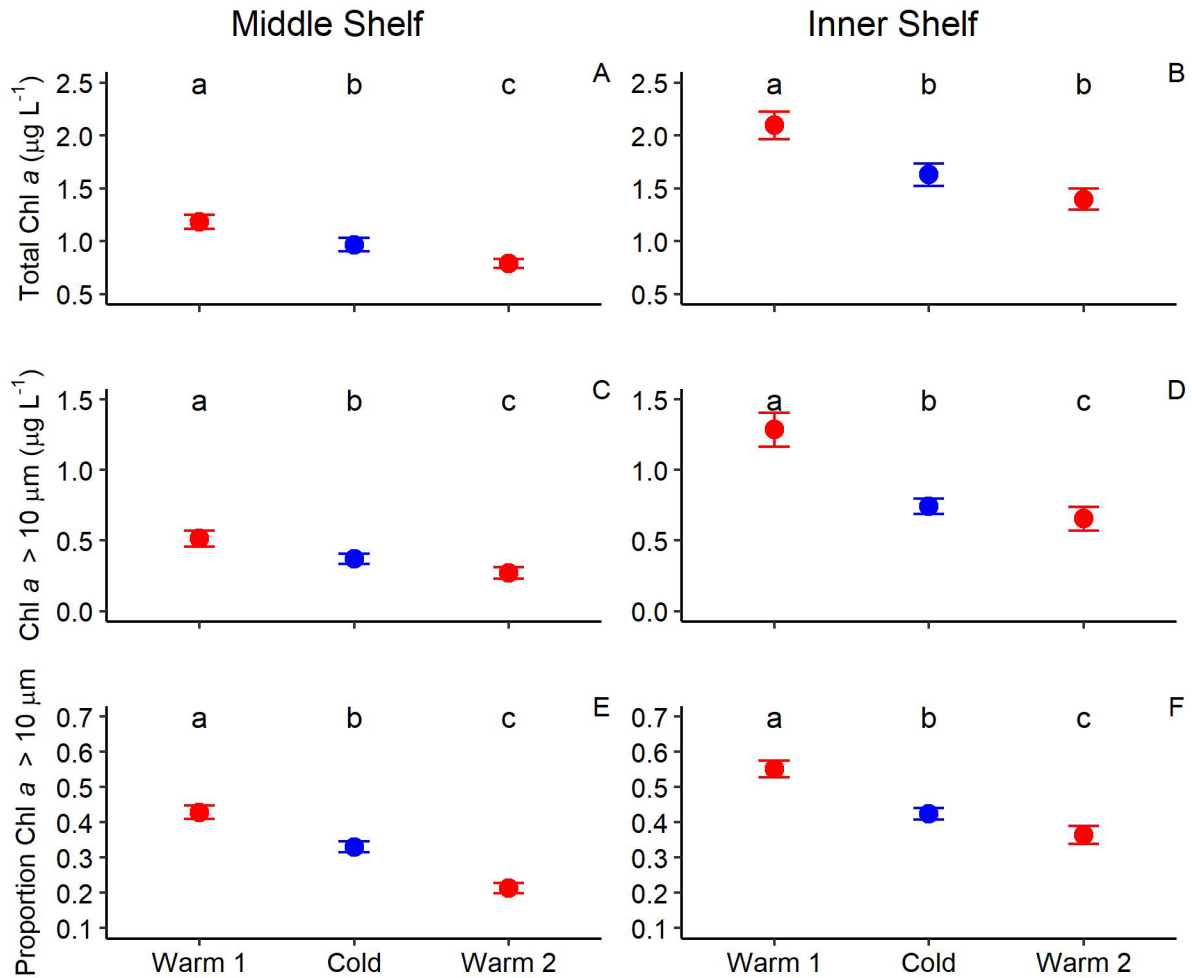
Figure 4. Comparisons of total chlorophyll *a* concentration (Total Chl *a*) (A, B), chlorophyll > 10 μm cell diameter concentration (Chl *a* > 10 μm) (C, D), and proportion of chlorophyll *a* > 10 μm (E, F) across Warm 1 (2002-2005, red), Warm 2 (2014-2018, red) and Cold (2006-2013, blue) for the middle (left panels) and inner shelf (right panels). Points represent time-period mean and error bars ± 1 SE of the mean (Middle: Warm 1 $N = 67$, Cold $N = 108$, Warm 2 $N = 140$; Inner: Warm 1 $N = 63$, Cold $N = 110$, Warm 2 $N = 81$). Periods that have different lower case letters had means that differed based on Kruskal-Wallis ($p < 0.05$) and Dunn's *post-hoc* tests ($p < 0.05$) and periods with the same lower case letter did not.
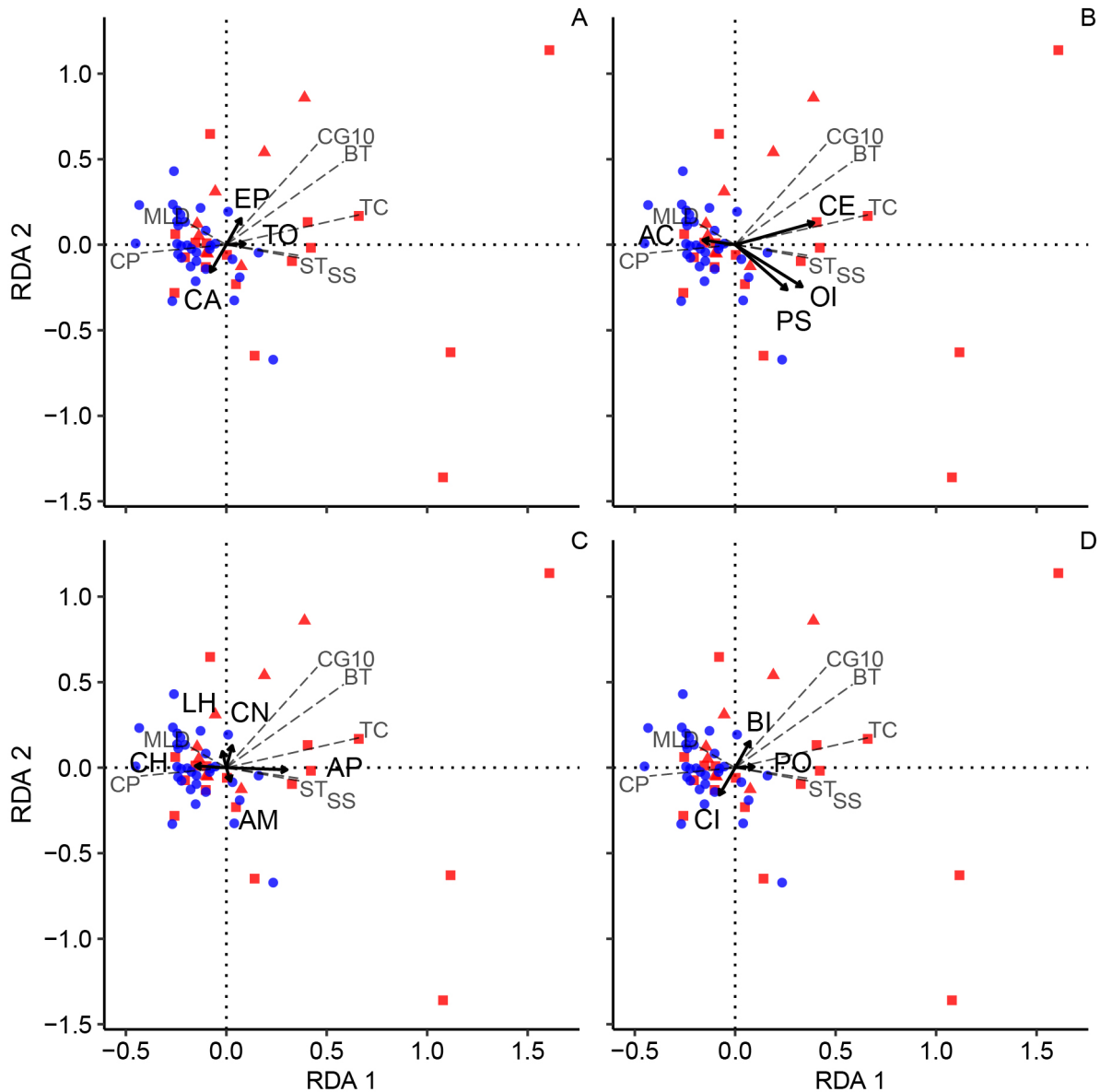
Figure 5. Redundancy analysis bi-plots for the middle shelf. Zooplankton taxa (black, solid line) were divided into four groups: Copepods > 2 mm (A), Copepods < 2 mm (B), Holoplankton (C), and Meroplankton (D). Taxa abbreviations and group membership are found in Table 3. Environmental variables (light gray, dashed line) abbreviations are found in Table 1. Each data point represents one sampling station; Warm 1 (2002-2005, red triangles), Warm 2 (2014-2018, red squares) and cold (2006-2013, blue circles).
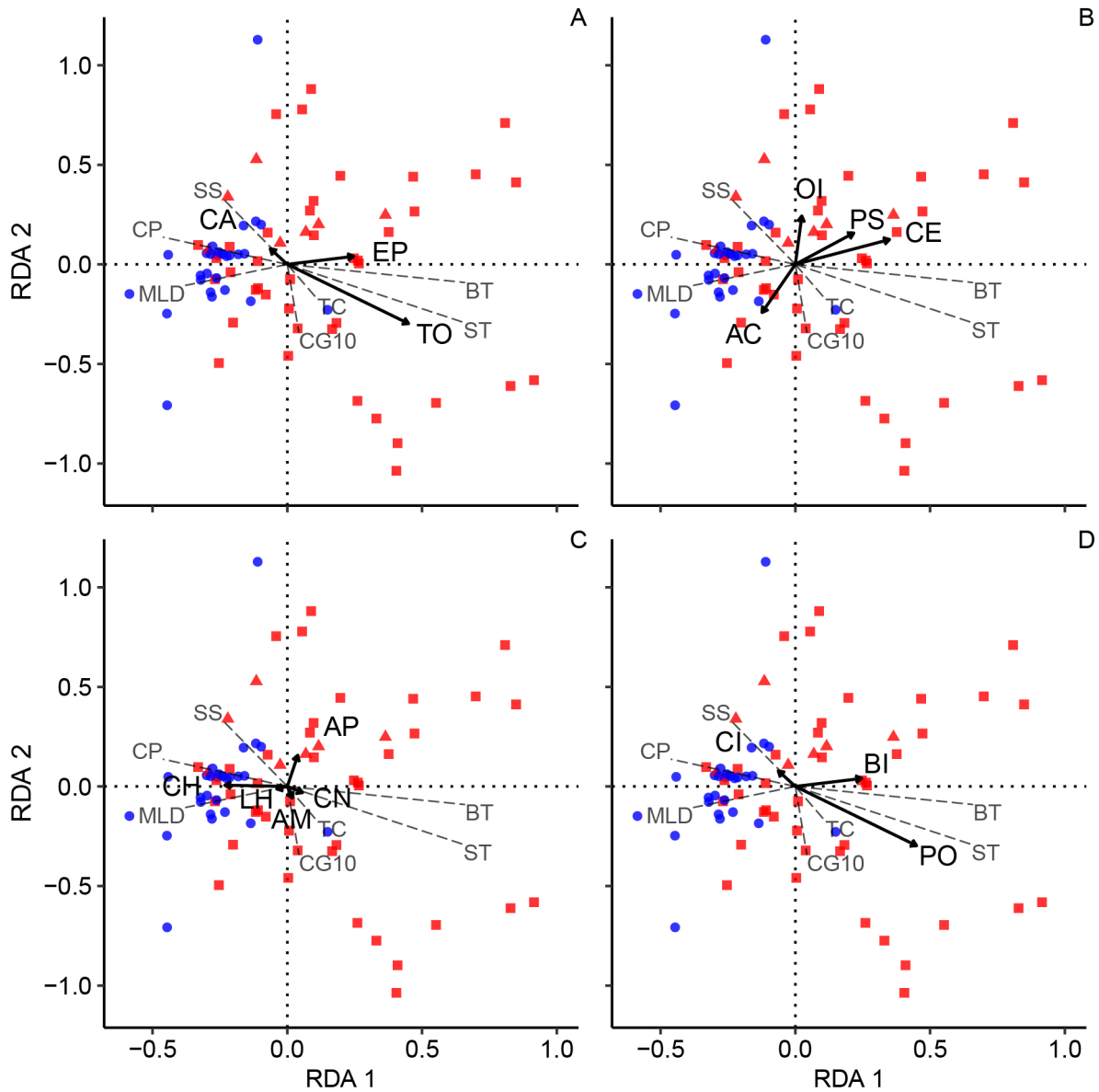
Figure 6. Redundancy analysis bi-plots for the inner shelf. Zooplankton taxa (black, solid line) were divided into four groups: Copepods > 2 mm (A), Copepods < 2 mm (B), Holoplankton (C), and Meroplankton (D). Taxa abbreviations and group membership are found in Table 3. Environmental variables (light gray, dashed line) abbreviations are found in Table 1. Each data point represents one sampling station; Warm 1 (2002-2005, red triangles), Warm 2 (2014-2018, red squares) and cold (2006-2013, blue circles).

1015
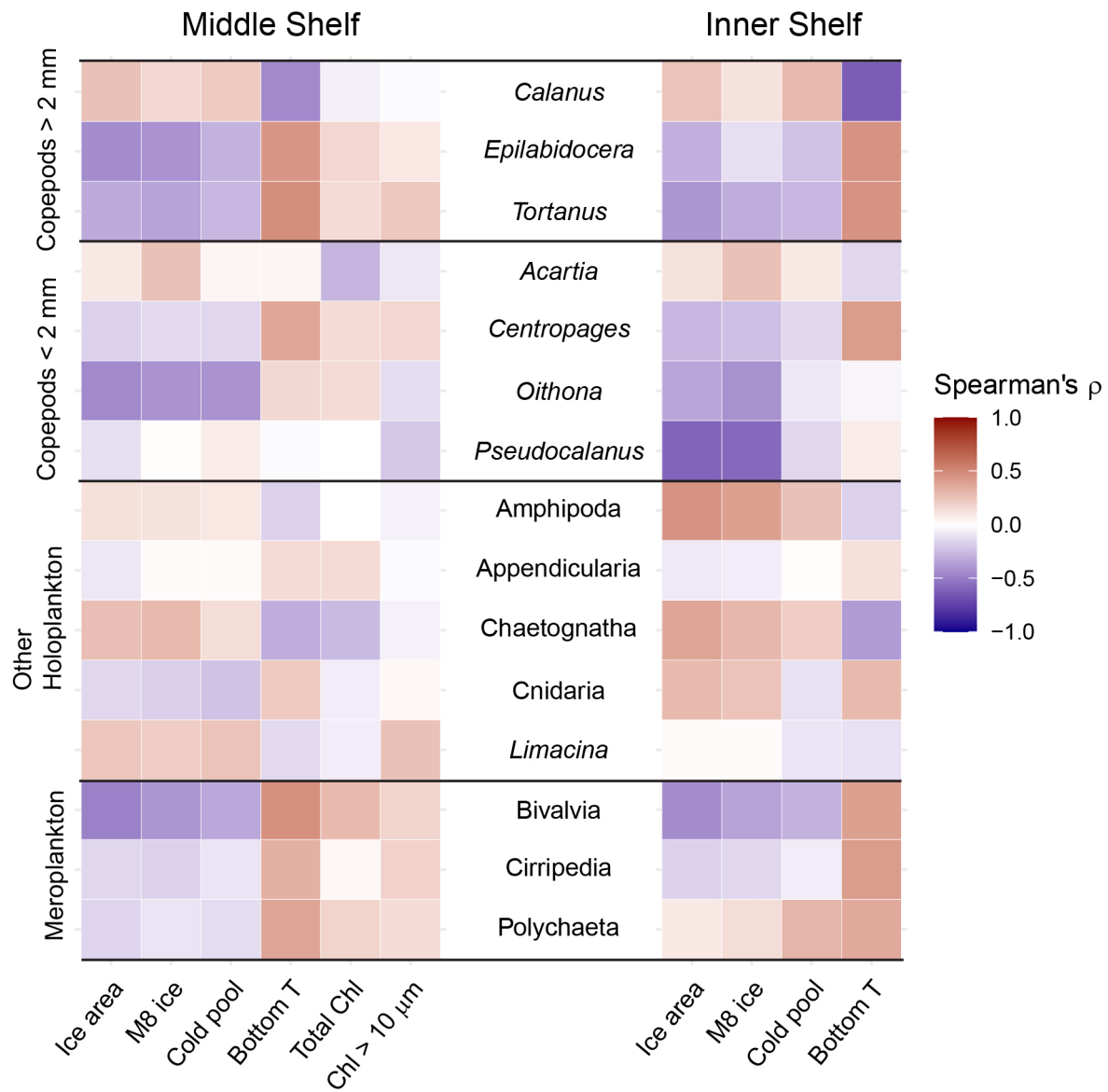
Figure 7. Correlation (Spearman's ρ) heat map for zooplankton identified by taxa and group and
environmental variables identified by step-wise model selection during redundancy analysis
(Table 4). Positive correlations are shown by the increasing intensity of red and negative
correlations by the increasing intensity of purple.
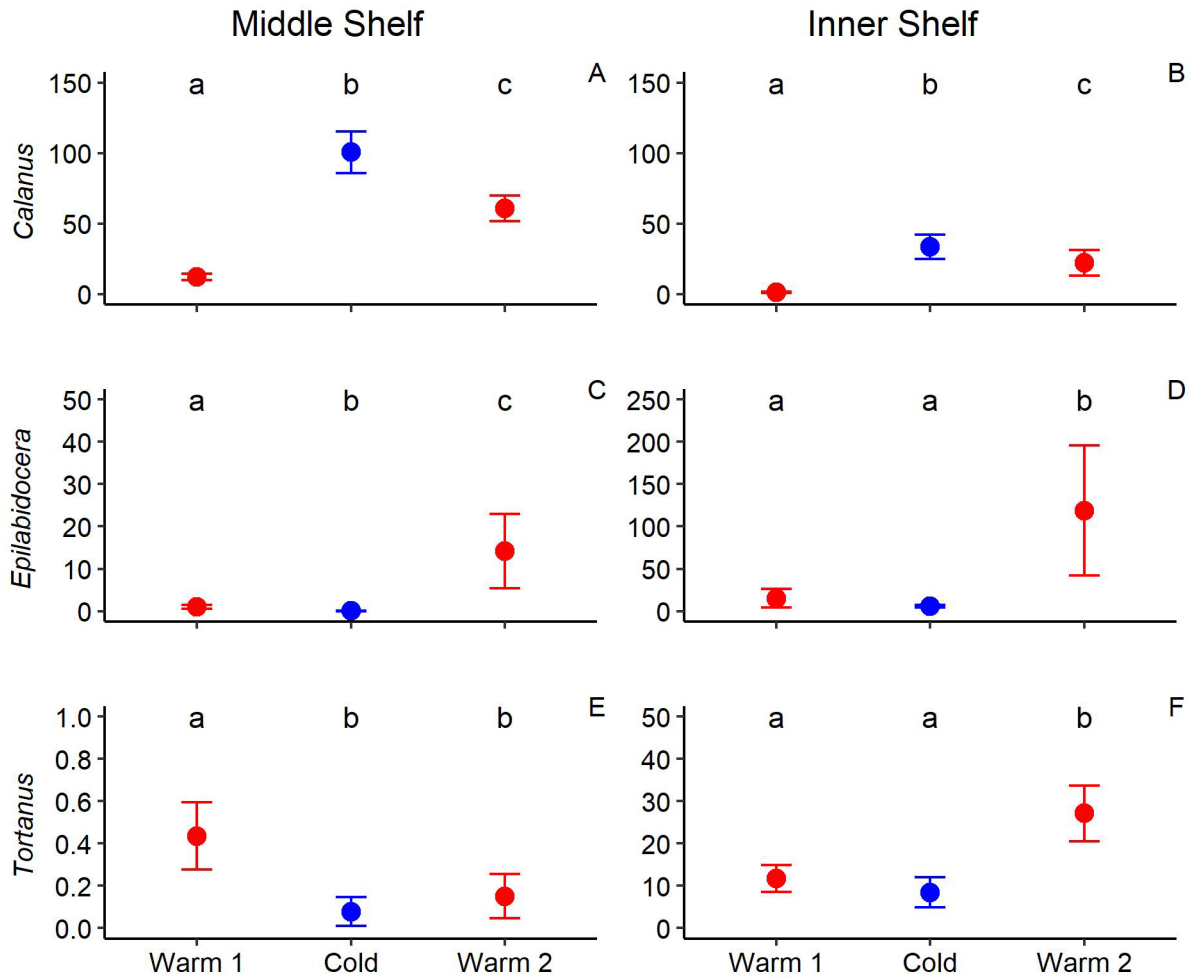
Figure 8: Copepods > 2 mm: Differences in abundance (number m^{-3}) of *Calanus* spp. (A, B), *Epilabidocera longipedata* (C, D), and *Tortanus discaudatus* (E, F) across Warm 1 (2002-2005, red), Warm 2 (2014-2018, red) and Cold (2006-2013, blue) for the middle (left panels) and inner shelf (right panels). Points represent time-period mean and error bars ± 1 SE of the mean (Middle: Warm 1 $N = 58$, Cold $N = 103$, Warm 2 $N = 83$; Inner: Warm 1 $N = 62$, Cold $N = 101$, Warm 2 $N = 81$). Periods that have different lower case letters had means that differed based on Kruskal-Wallis ($p < 0.05$) and Dunn's *post-hoc* tests ($p < 0.05$) and periods with the same lower case letter did not.
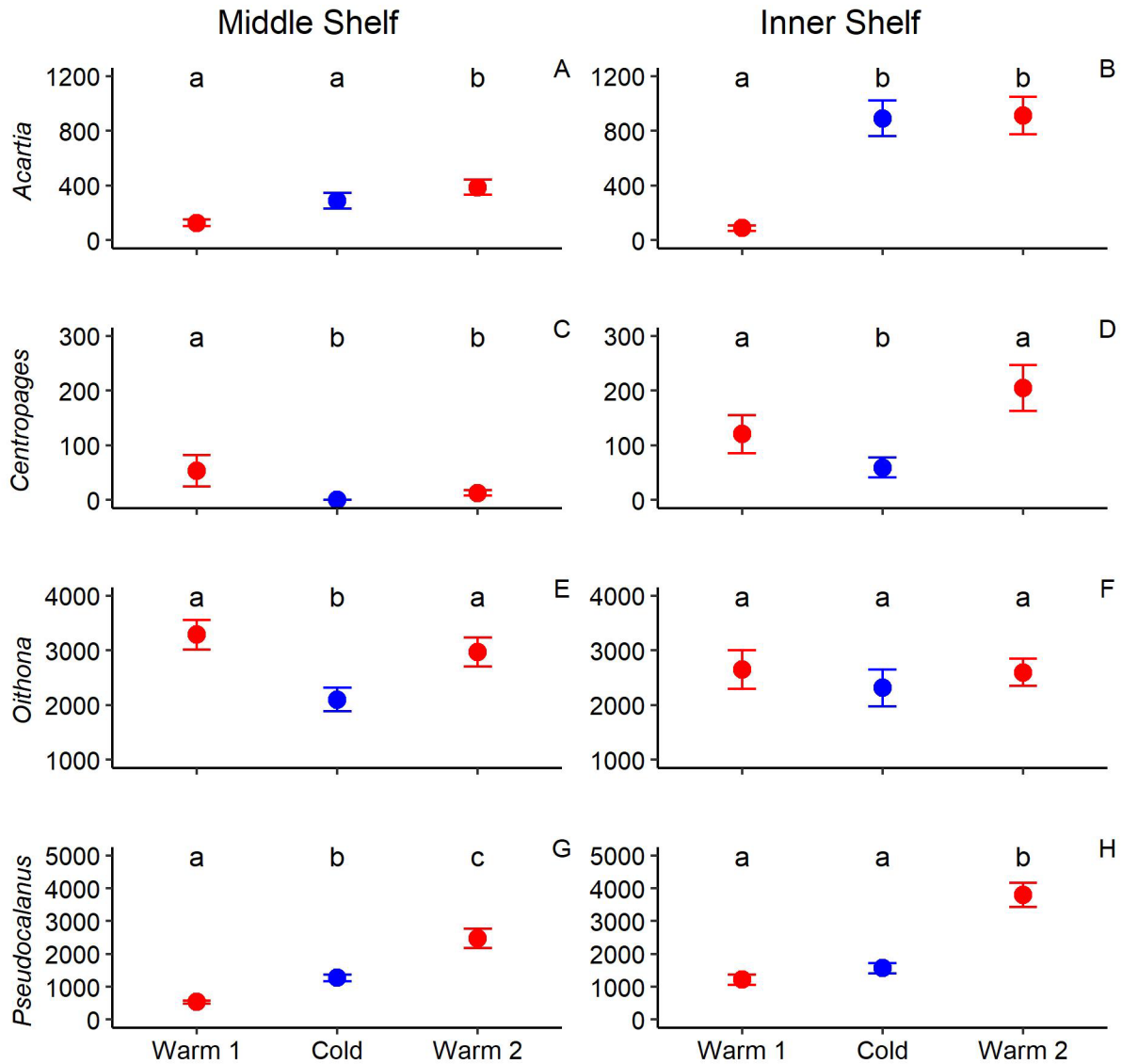
Figure 9. Copepods < 2 mm: Differences in abundance (number m^{-3}) of *Acartia* spp. (A, B), *Centropages abdominalis* (C, D), *Oithona* spp. (E, F), and *Pseudocalanus* spp. (G, H) across Warm 1 (2002-2005, red), Warm 2 (2014-2018, red) and Cold (2006-2013, blue) for the middle (left panels) and inner shelf (right panels). Points represent time-period mean and error bars ± 1 SE of the mean (Middle: Warm 1 $N = 58$, Cold $N = 103$, Warm 2 $N = 83$; Inner: Warm 1 $N = 62$, Cold $N = 101$, Warm 2 $N = 81$). Periods that have different lower case letters had means that differed based on Kruskal-Wallis ($p < 0.05$) and Dunn's *post-hoc* tests ($p < 0.05$) and periods with the same lower case letter did not.
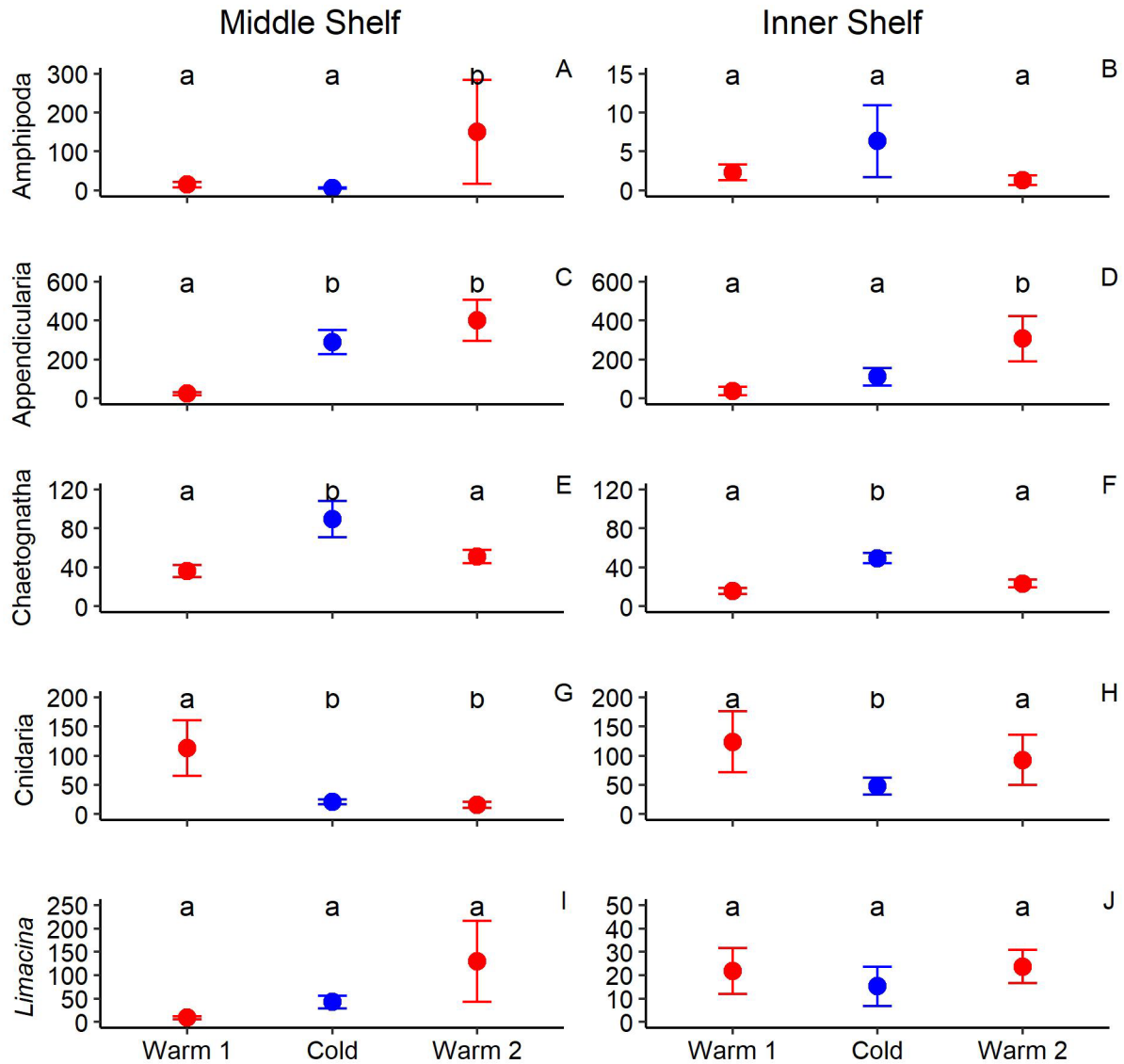
Figure 10: Other holoplankton: Differences in abundance (number m^{-3}) of Amphipoda (A, B), Appendicularia (C, D), Chaetognatha. (E, F), Cnidaria (G, H), and *Limacina helicina* (I, J) across Warm 1 (2002-2005, red), Warm 2 (2014-2018, red) and Cold (2006-2013, blue) for the middle and inner shelf. Points represent time-period mean and error bars ± 1 SE of the mean (Middle: Warm 1 $N = 58$, Cold $N = 103$, Warm 2 $N = 83$; Inner: Warm 1 $N = 62$, Cold $N = 101$, Warm 2 $N = 81$). Periods that have different lower case letters had means that differed based on Kruskal-Wallis ($p < 0.05$) and Dunn's *post-hoc* tests ($p < 0.05$) and periods with the same lower case letter did not.
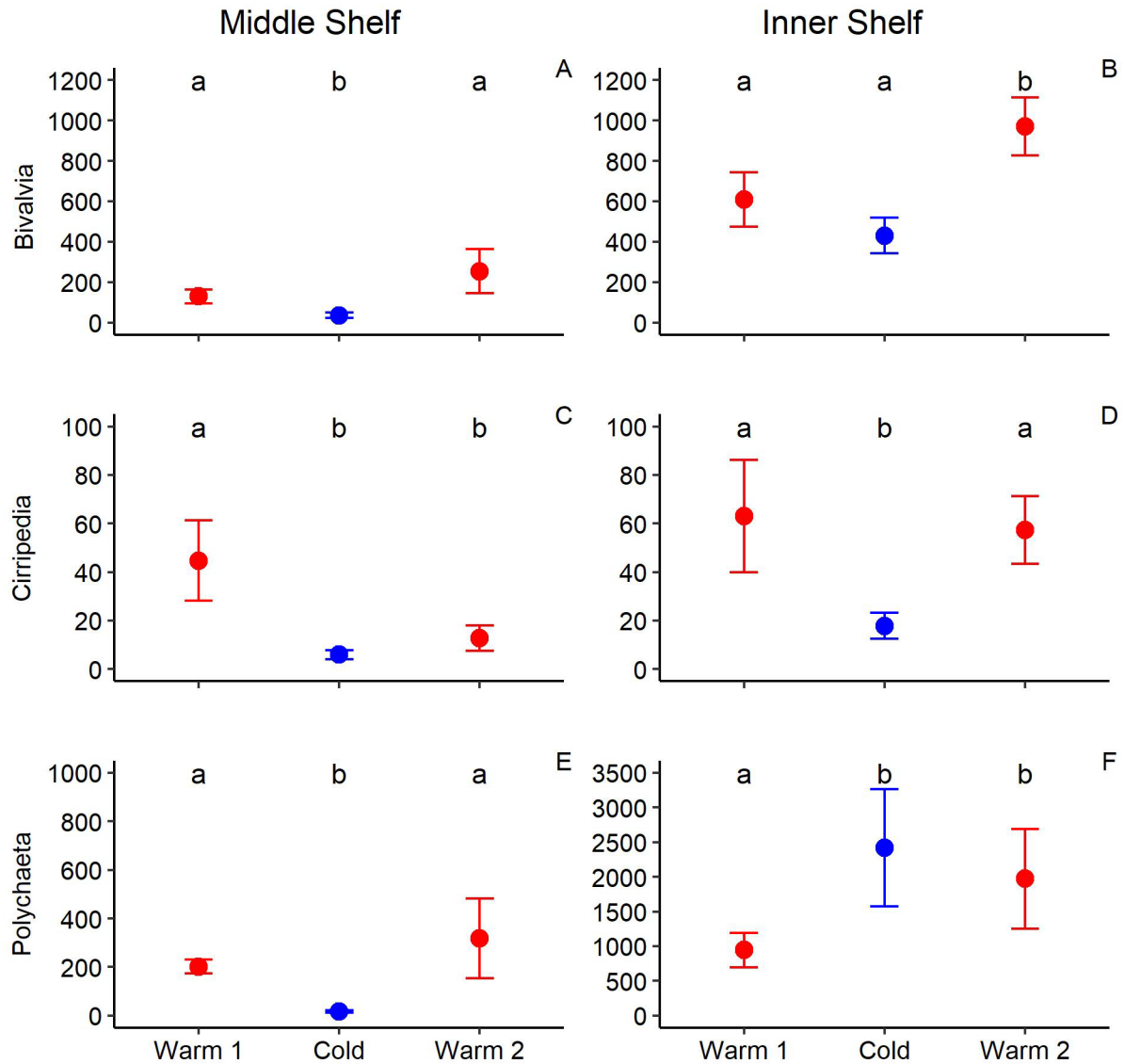
Figure 11: Meroplankton: Differences in abundance (number m^{-3}) of Bivalvia (A, B), Cirripedia (C, D), and Polychaeta (E, F) across Warm 1 (2002-2005, red), Warm 2 (2014-2018, red) and Cold (2006-2013, blue) for the middle and inner shelf. Points represent time-period mean and error bars ± 1 SE of the mean (Middle: Warm 1 $N = 58$, Cold $N = 103$, Warm 2 $N = 83$; Inner: Warm 1 $N = 62$, Cold $N = 101$, Warm 2 $N = 81$). Periods that have different lower case letters had means that differed based on Kruskal-Wallis ($p < 0.05$) and Dunn's *post-hoc* tests ($p < 0.05$) and periods with the same lower case letter did not.